People's Democratic Republic of Algeria
Ministry of Higher Education and Scientific Research

University M'Hamed BOUGARA – Boumerdes

Institute of Electrical and Electronic Engineering

Department of Electronics

Final Year Project Report Presented in Partial Fulfilment of the Requirements for the Degree of

MASTER

In **Power Engineering**

Option: **Power Engineering**

Title:

Reduced Number of Switch Direct Torque Control of Induction Machine with Bidirectional Capability

Presented by:

- **Aissou Ghilas**
- **Sklab Lainser**

Supervisor:

Dr. Metidji

Table of Contents

CHAPTER 03

SIMULATIONS AND RESULTS

Abstract

In the middle of 1980s a novel technic for alternating current (AC) machine control is proposed, this technic is known as direct torque control (DTC). It happens that the control algorithm of this technic is simple and less sensitive to machine parameters compared to others technics. It is based on direct determination of suitable switching states according to the error of the torque and flux. However, since the switching frequency of basic DTC is not constant then high torque and flux ripples are produced which in turns degrade the performance of this technic, especially at low speed regions.

This work introduces and compare between DTC or induction motor (IM) using six switch three phase inverter (SSTPI) and DTC for IM using four switch three phase inverter (FSTPI). The basic FSTPI results in four unbalanced voltage vectors, which in turns divide the αβ plane into four sectors. These unbalanced voltage vectors generated by the FSTPI leads to high torque and flux ripples, in order to improve these performances, effective vectors are introduced; this strategy is based on the emulation of the operation of the conventional SSTPI. This has been achieved by suitable combination of the four unbalanced voltage vectors. This approach allows using the well-known established switching table of SSTPI for FSTPI. The simulation results comparaison of the proposed FTSTPI fed IM drive with the conventional SSTPI system shows that the proposed technic is quite acceptable considering its performance such as fast speed response, cost reduction and other advantages features.

Acknowledgements

I would like to express my gratitude to our supervisor Dr. Metidji for his guidance, patience and insightful remark that made possible the completion of this project. We extend our thanks to the members of the jury for having accepted to examine our work.

Finally, we would like to thank family and friends for their valuable support.

List of Figures

List of Tables

General Introduction

In the past, direct current (DC) motors were used extensively in areas where variable speed operation was required, since their flux and torque could be controlled easily by the field and armature current. However, DC motors have certain disadvantages, which are due to the existence of the commutator and the brushes. That is, they require periodic maintenance. They cannot be used in explosive or corrosive environments and they have limited commutator capability under high-speed, high voltage operational conditions. These problems can be overcome by the application of alternating-current motors, which can have simple and rugged structure, high maintainability and economy. They are also robust and immune to heavy overloading. Their small dimension compared with DC motors allows AC motors to be designed with substantially higher output ratings for low weight and low rotating mass. The lower cost of AC motors has also been a decisive economic factor in multi-motor systems. However, as a result of the progress in the field of power electronics, the continuing trend is towards cheaper and more effective power converters, and single motor AC drives compete favorably on a purely economic basis with the DC drives (Bimal Bose 2002, Krishnan 2005).

Variable speed drives require variable voltage and frequency supply which is invariably obtained from a three phase voltage source inverter (VSI). In scalar control IM speed and torque can be controlled using inverters by regulating the voltage and frequency of the inverter output. The scalar control methods of IM drive is simple to implement but have the disadvantages of sluggish control response because of the inherent coupling effect in the machine and easily prone to instability.

There are two types of instantaneous electromagnetic torque-controlled drives used for high performance applications. The most used technics are field oriented control (FOC) and direct torque control (DTC) drives. FOC technique was introduced in Germany by Blaschke in 1968, FOC appeared to have similar performance to the DC machine over a wide range of speed and load conditions, but the performance of a FOC implementation depends critically on very accurate co-ordinate transformations and flux angle estimation, which are complex calculations and sensitive to variations in motor parameters. DTC technique was introduced in Japan by Takahashi in 1984, they have achieved a high degree of maturity and have become increasingly popular in a wide range of applications [1]. DTC strategy involves direct control

of the flux linkages (e.g. stator flux linkages, stator transient flux linkages, etc.) and electromagnetic torque by applying optimum current or voltage switching vectors of the inverter which supplies the motor.

The most frequently discussed and used power electronic converter in DTC drives is the VSI [11]. Commonly, the voltage source inverter (VSI) feeding IM under DTC is the six-switch three-phase inverter (SSTPI) but, some applications such as electric and hybrid propulsion systems should be as reliable as possible. Within this requirement, the reconfiguration of the SSTPI into a four-switch three phase inverter (FSTPI), in case of a switch/leg failure is recommended, also for industrial application a FSTPI is more economical then a SSTPI and this very important from the economical point of view.

This work examines and compares between direct torque control (DTC) strategy for induction motor (IM) drives fed by a six switch three-phase inverter (SSTPI) and four switch three-phase inverter (FSTPI).This research work is addressing four principal points:

i. Development and simulation of two switch PWM rectifier.

ii. To develop MATLAB/SMULINK package for direct torque control of induction motor (DTC) model fed by :

- ✓ Six switch three phase inverter (SSTPI)
- ✓ Basic four switch three phase inverter (FSTPI)
- ✓ Four switch inverter emulating six switch inverter operation

iii. Evaluation of different developed DTC models under the torque/speed control modes (four quadrant operation).

iv. Comparison between different DTC developed models.

The main body of the work is structured as follows:

The first chapter summarizes a background about different control strategies of the induction motor, like the classical methods (the scalar and the vector control) and DTC which take the most of our interest.

The second chapter discusses the working principle and the control scheme of PWM rectifier and DTC based SSTPI, FSTPI and enhanced FSTPI.

The third chapter discusses the simulation result of the PWM and the DTC control technics.

CHAPTER 1

REVIEW OF DIFFERENT CONTROL STRATEGIES OF IM

1.1. Introduction

Traditionally, the induction motor has been operated directly from the grid with fixed speed/frequency (50Hz/60Hz), but since the development of the power electronic converts, it can be used now in variable frequency by inserting a converter between the motor and the electrical grid. This makes it possible to obtain an adjustable speed motor [13].

The variable frequency drives (VFDs) are able to provide smoother speed tuning and greater motor control. To control the speed, the torque and the position, various AC drives control strategies have been developed over the years. They can be classified based on their principles into two main categories namely by the scalar and vector control methods. The scalar control is developed by the steady state model of the machine (per phase equivalent circuit model), where only the magnitude and frequency of voltage, current, and flux can be controlled [14]. Thus, it does not operate on the space vector position during the transient state. Contrariwise, the vector control is developed in the dynamic states, more than the magnitudes, the instantaneous positions of voltage, current, and flux can be controlled [15].

1.2. CONTROL SCHEMES OF INDUCTION MOTOR

1.2.1. Scalar control

The Scalar control (*V/f*) which is known also by Volt/Hertz control is a simple technique used to control the speed the induction Motors. The main concept of *V/f* method is to keep the ratio of the stator voltage to frequency constant to maintain constant maximum available torque. To control speed is in a closed loop, a proportional integral controller (PI) is employed to maintain the speed at a desired value and to improve speed accuracy by regulating slip speed of the motor. The controller receives the speed tracking error which is the difference between the desired reference ω_{r*} and the actual sensed rotor speed ω_r as described in **Figure.1.1.**

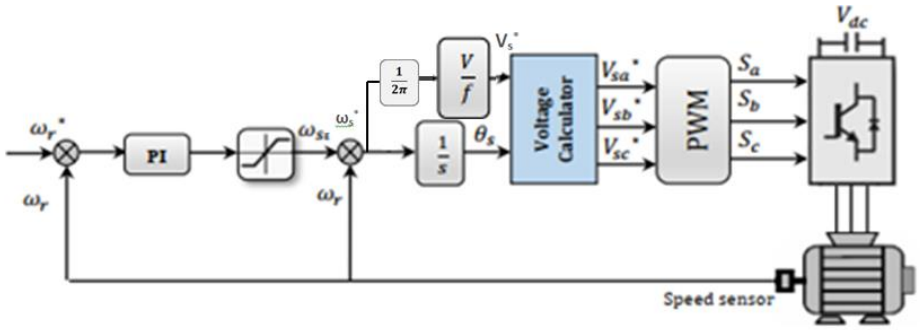

Figure.1.1 Closed loop scalar control for variable frequency induction motor drive.

This technique can operate in open loop also (i.e. without speed feedback), however, it provides poor speed regulation which is become depended on the applied external load [20]. The main drawbacks of this technique are the unsatisfied speed accuracy. In addition, the sluggish dynamic response which produce slow torque response. Since the control design is maintained in the steady state, the magnitude of the stator flux is not controlled during the transient and the machine's torque cannot respond quickly [21].

1.2.2. Field Oriented Control (FOC)

The use of induction motors at its highest efficiency is a challenging task because of their complex mathematical model and non-linear characteristic during saturation. These factors make the control of induction motor difficult and call for use of a high performance control algorithms such as "vector control". Scalar control such as the "V/Hz" strategy has its limitations in terms of performance. The scalar control method for induction motors generates oscillations on the produced torque due to the deviation of air gap flux linkages from their reference values. Hence to achieve better dynamic performance, a more superior control scheme is needed for Induction Motor. With the mathematical processing capabilities offered by the microcontrollers, digital signal processors and FGPA, advanced control strategies can be implemented to decouple the torque generation and the magnetization functions in an AC induction motor. This decoupled torque and magnetization flux is commonly called rotor Flux Oriented Control (FOC).

Field Oriented Control (FOC) is probably the most common control method used for high-performance induction motor applications. The invention of FOC in the beginning of 1970s, and the demonstration that an induction motor can be controlled like a separately excited DC motor, brought a renaissance in the high-performance control of ac drives. Because of dc machine-like performance, FOC is also known as decoupling, orthogonal, or transvector control. FOC was the first technique developed to allow independent control of induction motor torque and flux. It refers to induction motor operation in a synchronously rotating *dq* reference frame that is aligned with one of the motor fluxes typically the rotor flux. In this mode of operation, control of the torque and flux is decoupled such that the *d*-axis component of the stator current controls the rotor flux magnitude and the *q*-axis component controls the torque produced. This was initially difficult to implement due to the complexity of transforming the three phase variables to a rotating (*d, q)* reference frame. With the

development of suitable low cost microprocessors in the early 1980s, FOC become practical to implement in commercial motor drives. The general block diagram of the indirect field orientation control for an induction motor is shown in **Figure.1.2**

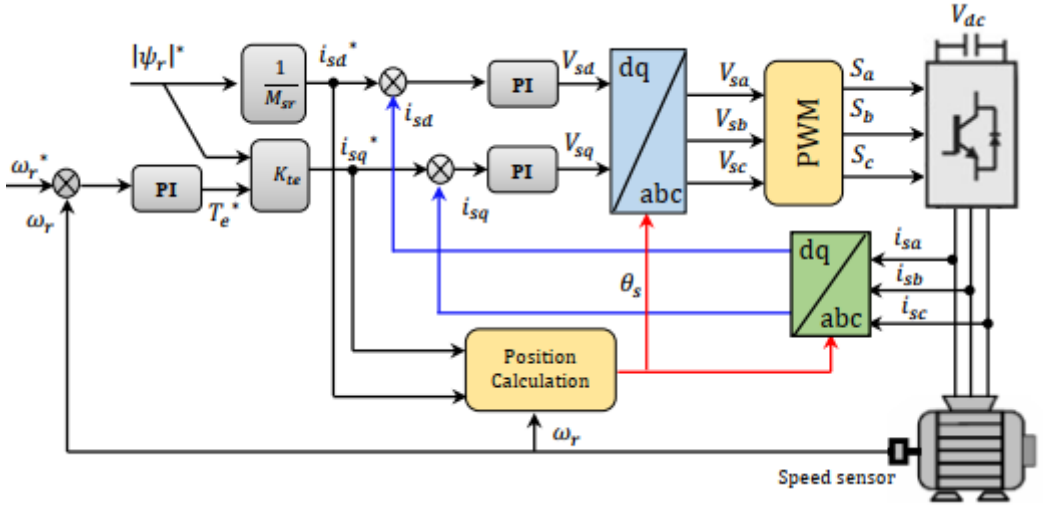

Figure.1.2 Basic indirect field oriented control (IFOC) of induction motor.

1.2.2.1. Working Principle of Field Oriented Control

The field oriented control consists of controlling the stator currents represented by a vector. This control is based on projections that transform a three phase time and speed dependent system into a two coordinate (d and q frame) time invariant system. These transformations and projections lead to a structure similar to that of a DC machine control. FOC machines need two constants as input references: the torque component and the flux component.

The torque *Te* developed by the induction motor is given by Eqs (A.35) and (A.36) as:

$$T_e = \frac{3}{2}\frac{p}{2}\left(\psi_{ds} i_{qs} - \psi_{qs} i_{ds}\right) = \frac{3}{2}\frac{p}{2}\frac{L_m}{L_r}\left(\psi_{dr} i_{qs} - \psi_{qr} i_{ds}\right) \quad (1.1)$$

To make the torque equation looks like that of the DC machine, the second term must be null. This can be achieved by aligning the d-axis of the rotating reference frame (dq) with the rotor flux axis (ψ_r) or the stator flux axis (ψ_s). And this is why the technique called Field-Oriented Control.

Therefore, the flux to which the d-axis is oriented, determines the type of the controller whether it is **rotor-field oriented** controller or **stator-field oriented** controller as shown in **Figure.1.3**.

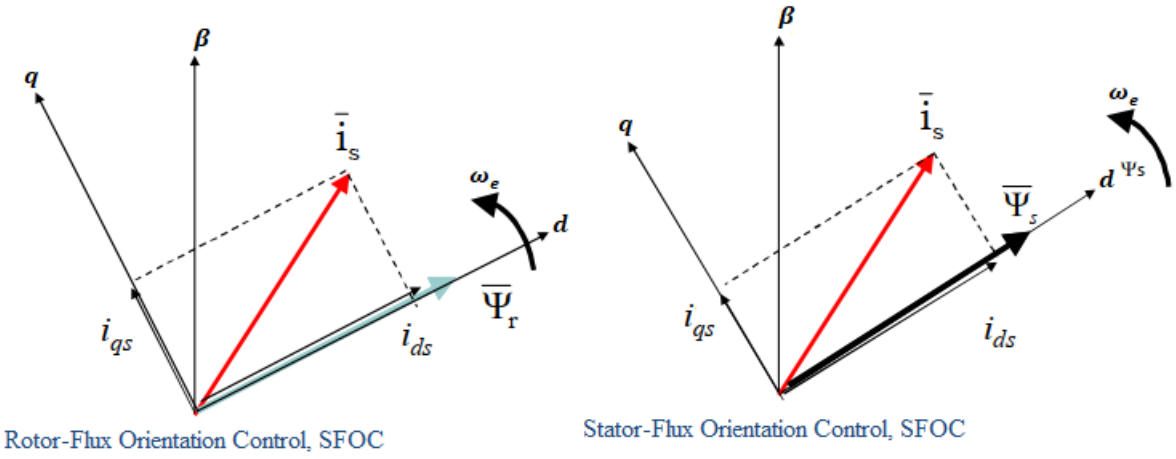

Figure.1.3 Orientation of *d*-axis of *dq* rotating frame toward the flux ψ_r and ψ_s

- For RFOC the torque equation becomes:

$$T_e = \frac{3}{2}\frac{p}{2}\frac{L_m}{L_r}\left(\psi_{dr} i_{qs} - \psi_{qr} i_{ds}\right) = \frac{3}{2}\frac{p}{2}\frac{L_m}{L_r}\psi_{dr} i_{qs} \qquad (1.2)$$

- For SFOC the torque equation becomes:

$$T_e = \frac{3}{2}\frac{p}{2}\left(\psi_{ds} i_{qs} - \psi_{qs} i_{ds}\right) = \frac{3}{2}\frac{p}{2}\psi_{ds} i_{qs} \qquad (1.3)$$

The most used is rotor-field oriented control. By orienting the d-axis toward the rotor flux, the torque can be controlled by the component i_{qs} whereas the flux can be controlled by the i_{ds} component. Because of the orthogonal orientation of these components the torque and the flux can be controlled independently.

1.2.2.2. Classification of Field Oriented Control

FOC for the induction motor drive can be broadly classified into two types: Indirect FOC and Direct FOC schemes. In DFOC strategy rotor flux vector is either measured by means of a flux sensor mounted in the airgap or by using the voltage equations starting from the electrical machine parameters. But in case of IFOC rotor flux vector is estimated using the field oriented control equations (current model) requiring a rotor speed measurement. Among both schemes, IFOC is more commonly used because in closed-loop mode it can easily operate throughout the speed range from zero speed to high-speed field-weakening.

1.2.2.3. Advantages of Field Oriented Control

- Improved torque response
- Torque control at low frequencies and low speed

- Dynamic speed accuracy
- Reduction in size of motor, cost and power consumption
- Four quadrant operation
- Short-term overload capability

1.2.2.4. Disadvantages of Field Oriented Control

- FOC has several disadvantages, the most significant being the necessity to use a speed sensor. This can be implemented mechanically or as a complex software sensor (observer). The sensor is needed because FOC must determine the exact rotor position in order to generate an appropriate magnetic field in the stator for maximum torque.
- The use of sensors and observers, however, leads to increasing costs and a higher error rate especially in vehicle applications.
- According to e-Traction, a Dutch manufacturer of motors for electric busses, FOC sensors turned out to be the most unreliable parts of the entire system setup.
- The company reports that most motor failures could be attributed to difficulties with these sensors.

1.2.3. Direct Torque control (DTC)

The name direct torque control is derived by the fact that, on the basis of the errors between the reference and the estimated values of torque and flux, it is possible to directly control the inverter states in order to reduce the torque and flux errors within the prefixed band limits. Unlike FOC, DTC does not require any current regulator, coordinate transformation and PWM signals generator (as a consequence timers are not required). In spite of its simplicity, DTC allows a good torque control in steady-state and transient operating conditions to be obtained. The problem is to quantify how good the torque control is with respect to FOC. In addition, this controller is very little sensible to the parameters detuning in comparison with FOC.

1.2.3.1. Reasons for selecting DTC

Many researches have been carried out to try to solve induction motor control (Boldea and Nasar 1988, Casadei et al 1993, Casadei et al 1994, Tiitinen 1995, Nash 1997, Casadei et al 1998, Habetler et al 1992…). In particular the following solutions have been developed:

- Use of improved switching tables.
- Use of comparators with and without hysteresis, at two or three levels.

- implementation of DTC schemes for constant switching frequency operation with PWM or SVM techniques
- Implementation of DTC schemes for constant switching frequency operation with PWM or SVM techniques
- Use of sophisticated flux estimators to improve the low speed behavior

The DTC scheme is characterized (in comparison with the DFOC) by the absence of:

- Coordinate transformations
- Current regulators
- PWM signal generators (no timers)

So, only the control schemes, which meet all these requirements, should be considered as real DTC schemes. According to these considerations, the analysis is carried out with reference to a basic DTC scheme characterized by the above mentioned features.

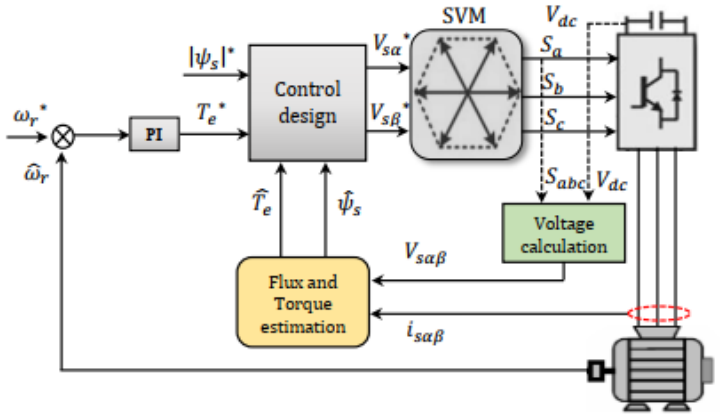

Figure.1.4 Block diagram of conventional direct torque control scheme

Figure.1.4 shows a block diagram of the direct torque control scheme. The estimated stator flux magnitude and torque are compared to the reference values. A single voltage vector is then selected that will drive the error in both parameters to zero. The optimal switch states are supplied to the PWM inverter that drives the induction motor. The disadvantage of conventional DTC is the high torque and flux ripple and high current distortion.

1.3. Conclusion:

Among different Control strategies of electric machines that affect the whole system performance. The DTC overcome the major drawback of FOC which is the use of speed sensor and complex observers. In addition to the realization simplicity of the DTC control strategy.

CHAPTER 2

DIRECT TORQUE CONTROL METHODS FOR THE INDUCTION MOTOR

2.1. Introduction

In the past, researchers mainly concentrated on the development of the efficient control algorithms for high performance variable speed IM drives However, the cost, simplicity and flexibility of the overall drive system which become some of the most important factors did not get that much attention to the researchers. That's why, despite tremendous research in this area most of the developed control system failed to attract the industry.

In this chapter, a six switch three phase inverter (SSTPI) fed IM as well as four switch three phase inverter drives are developed. The block diagram of the investigated DTC control technique with power flow capability is shown in **Figure.2.1**. It uses only six switches instead of ten; two switches for the rectifier and four switches for the inverter this make the technique cost-effective, less switching losses, less chances of destroying the switches due to lesser interaction among switches, less complexity of control algorithms and interface circuits as compared to the conventional SSTP inverter, the proposed control approach reduces the computation for real time implementations.

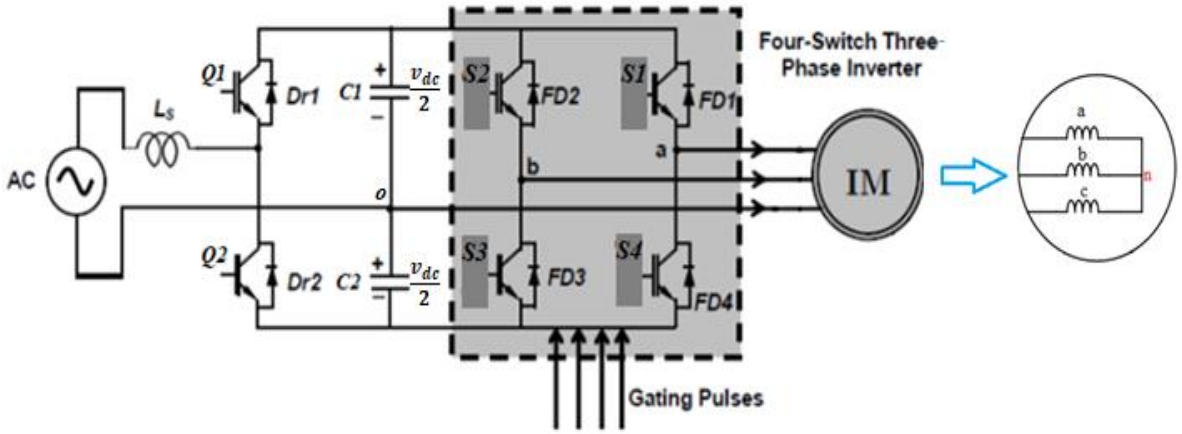

Figure.2.1 block diagram of the investigated DTC control technique

2.2. Model of Induction Motor Dedicated for Direct Torque Control

The dynamic equation's model of the induction motor which is dedicated for direct torque control is expressed below in Eq (2.1) and Eq (2.2). It can be written in the stator fixed reference frame (α,β) (stationary frame) by assuming the stator current and the stator flux as state variables.

$$\frac{di_{\alpha s}}{dt} = -\left(\frac{R_s}{\sigma L_s} + \frac{R_r}{\sigma L_r}\right) i_{\alpha s} + \omega_r i_{\beta s} + \frac{R_s}{\sigma L_s L_r}\psi_{\alpha s} - \frac{\omega_r}{\sigma L_r}\psi_{\beta s} + \frac{1}{\sigma L_s} v_{\alpha s} \quad (2.1)$$

$$\frac{di_{\beta s}}{dt} = -\left(\frac{R_s}{\sigma L_s} + \frac{R_r}{\sigma L_r}\right) i_{\beta s} - \omega_r i_{\alpha s} + \frac{R_s}{\sigma L_s L_r} \psi_{\beta s} + \frac{\omega_r}{\sigma L_r} \psi_{\alpha s} + \frac{1}{\sigma L_s} v_{\beta s} \quad (2.2)$$

$$\frac{d\psi_{\alpha s}}{dt} = v_{\alpha s} - R_s i_{\alpha s} \quad (2.3)$$

$$\frac{d\psi_{\beta s}}{dt} = v_{\beta s} - R_s i_{\beta s} \quad (2.4)$$

Where:

$i_{\alpha s}, i_{\beta s}$ are stator current components.

$\psi_{\alpha s}, \psi_{\beta s}$ are stator flux components.

R_s, R_r are stator and rotor resistance.

L_s, L_r are stator and rotor inductance.

$\sigma = 1 - \frac{M_{sr}}{L_s L_r}$ is the Blondel's coefficient.

M_{sr} is the mutual stator-rotor inductance.

2.3. Design and control of single phase PWM rectifier using two IGBTs

In Present days for AC-DC conversion we use SCR based phase controlled rectifier. This method is simple as we do not require any closed loop control and the required output voltage can be controlled. But looking at the source side, the phase controlled rectifier is drawing non sinusoidal current from the supply. In previous days we do not have any alternative method to handle this problem, but now using PWM rectifier we can be able to control both input side AC source current and the output side load voltage.

2.3.1. Power circuit and working principal

Figure.2.1 shows the power circuit of the single phase PWM rectifier also known as voltage doubler rectifier and boost rectifier. This topology uses only two power switches T_1 and T_2 and allows the four quadrants operation for the rectifier (**Figure.2.6**), which are switched complementary to control the dc-link voltage and the input current, but requires two filter capacitors C_1 and C_2, The voltage on each capacitor (Vc_1 and Vc_2) must be higher than the peak value of Vs to ensure the control of the input current, **Figure.2.5** gives the waveform of the input current and voltage. The possible combinations are as follows:

i. Switch T_1 is in the ON state (**Figure.2.3**) $\Rightarrow v_{AFE} = -V_{C2}$ so, the inductor voltage is

$$v_L = L\frac{di_s}{dt} = v_s(t) - V_{c1} < 0 \quad (2.5)$$

As v_L is negative, the input current will decrease its value.

ii. Switch T_2 is in the ON state (**Figure.2.4**) $\Rightarrow v_{AFE} = -V_{C2}$ so, the inductor voltage is

$$v_L = L\frac{di_s}{dt} = v_s(t) + V_{c2} > 0 \quad (2.6)$$

As v_L is positive, the input current will increase its value. Therefore, the waveform of the input current can be controlled by switching appropriately the power switches T_1 and T_2.

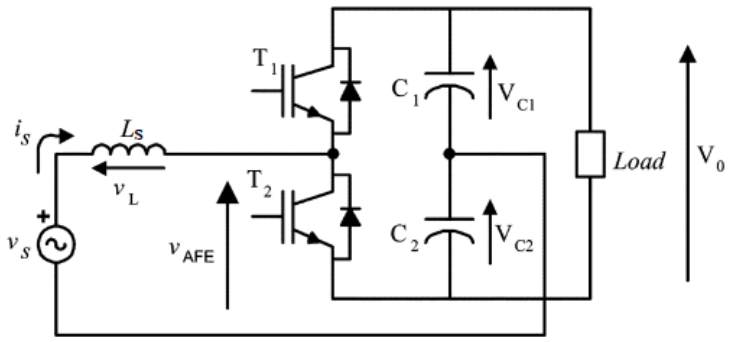

Figure.2.2 Single-phase PWM rectifier

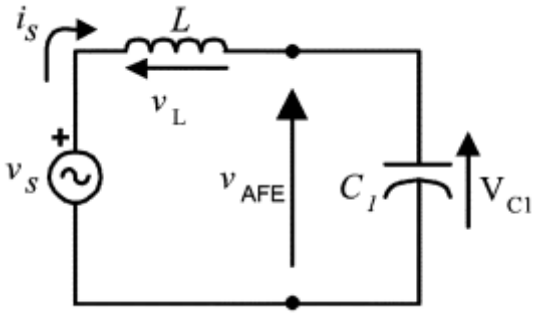

Figure.2.3 Equivalent circuit with T_1 ON

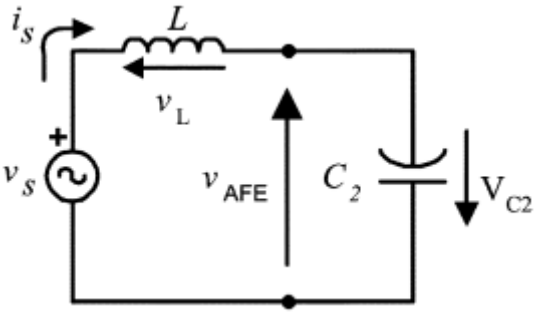

Figure.2.4 Equivalent circuit with T_2 ON

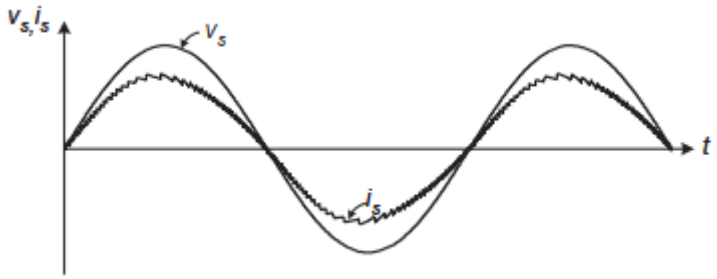

Figure.2.5 Waveform of the input current in the voltage doubler rectifier

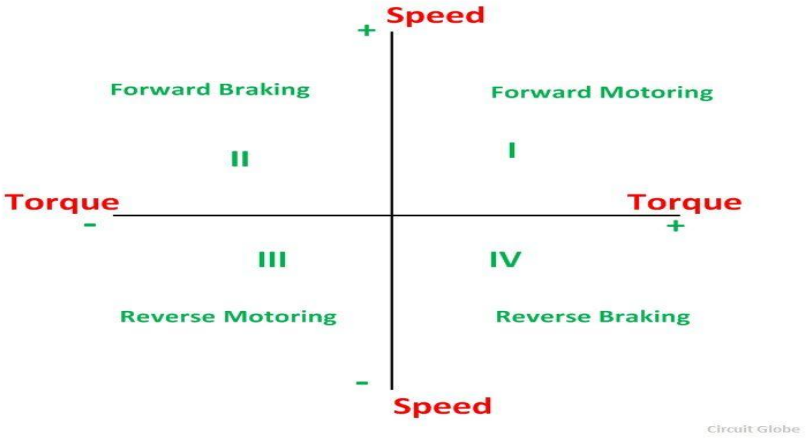

Figure.2.6 Four quadrant operation

2.3.2. Control scheme

The control scheme is shown in **Figure.2.7**. The control circuit should perform two controls:

1. Source current
2. Output voltage

Output of PI controller decides the magnitude of current to be drawn from the source which depends on the required reference voltage. From the source voltage, unit sine template is obtained and the reference current is obtained by multiplying the required magnitude of current and unit sine template. Hence the reference source current is obtained. The actual current through the inductor (actual source current) is controlled using hysteresis current controller method (**Figure.2.8**).

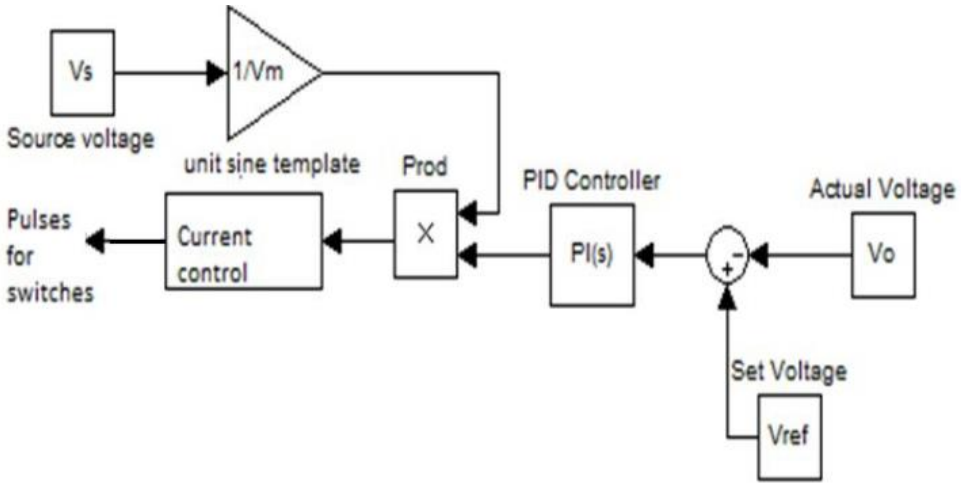

Figure.2.7 Control circuit for rectifier

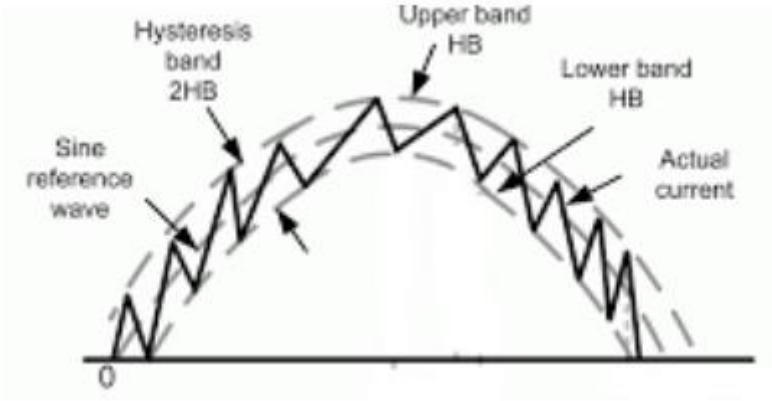

Figure.2.8 Hysteresis current control of inductor current

2.4. DTC based six switch inverter

2.4.1. Three phase voltage source inverter (VSI)

Before we move to the basic DTC algorithm, we should represent the model of the three-phase VSI. The power circuit topology of a three-phase voltage source inverter is shown in **Figure.2.9,** the induction motor is supposed as a star-connected three phase balanced load. Each power switch is a transistor, IGBT or a MOSFET with anti-parallel diodes. The pole or the leg voltages are denoted by a capital suffix letter V_a, V_b, V_c and can attain the value of 0.5 V_{dc} when the upper switch is operating and -0.5 V_{dc} when the lower switch is operating. The phase voltage applied to the load is denoted by the letters v_{an}, v_{bn}, v_{cn}. The operation of the upper and the lower switches are complimentary (a small dead band is provided in real time implementation). The induction motor is supposed as a star-connected three phase balanced load.

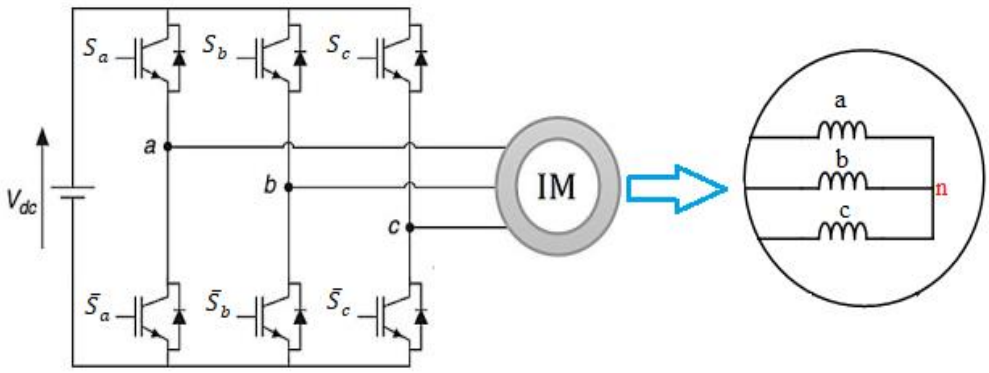

Figure.2.9 Three-phase VSI fed star-connected induction machine.

The relationship between the leg voltage and switching signals are

$$V_k = S_k V_{dc}; \quad k \in a, b, c \tag{2.7}$$

Where $S_k = 1$ when the upper power switch is 'ON' and $S_k = 0$ when the lower switch is 'ON.'

The voltage vector is generated by the following equation [22]:

$$V_s = \frac{2}{3} V_{dc} \left[S_a + S_b e^{j\frac{2\pi}{3}} + S_c e^{j\frac{4\pi}{3}} \right] \tag{2.8}$$

Where V_{dc} is the dc link voltage.

Since there are 3 switches S_a, S_b and S_c that controls the output voltage, then there exists 2^3=8 possible positions of the voltage space vector from the combination of the switching states, in which we distinguish six active vectors (V_1,V_2,V_3,V_4,V_5,V_6) and two zero vectors (V_0,V_7) [23]. The eight switching states are shown as space vectors in **Figure.2.10**:

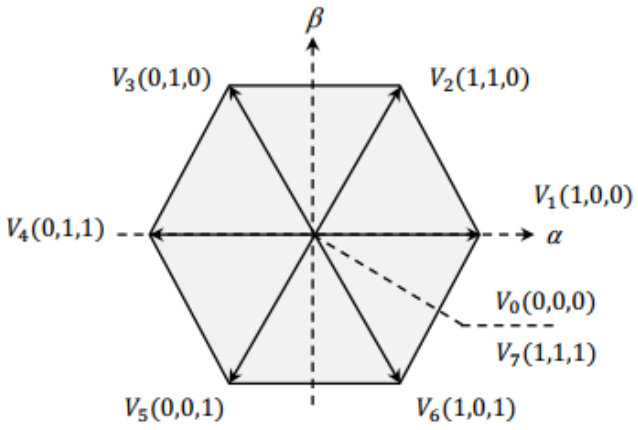

Figure.2.10 VSI Voltage vectors in the complex plane.

2.4.2. Basic Concept and Principles of DTC

Direct torque control achieves a decoupled control of the stator flux and the electromagnetic torque in the stationary frame (α, β). It uses a switching table for the selection of an appropriate voltage vector.

DTC requires set points of flux and torque as independent inputs it is then compared to the estimated quantities (flux and torque) an error signal is generated and then fed to two-level or three-level hysteresis controllers which determines whether an increase or a decrease of flux and/or torque is required, depending on whether or not torque or flux errors fall outside the predefined ranges. From this information, together with the knowledge of the position of the stator flux linkage space vector, an appropriate voltage vector will be selected based on the switching strategy. An accurate knowledge of the magnitude of the stator flux linkage space vector in the machine is needed. However, knowledge of the precise value of the stator flux space vector instantaneous position is not required. The control system only needs to know in which sector of the voltage vector space, which is a two-dimensional complex plane, the flux linkage space vector is [24].

2.4.3. Control of stator flux and electromagnetic torque

2.4.3.1. Stator flux control

Based on the IM model in the stationary reference frame, the stator voltage equation is given by

$$\frac{d\psi_s}{dt} = v_s - R_s i_s \tag{2.9}$$

If stator resistance voltage drop is neglected, the stator voltage equation in the stationary reference frame become

$$v_s = \frac{d\psi_s}{dt} \tag{2.10}$$

Hence the applied voltage directly empresses the stator flux. If the voltage abruptly changes, then the stator flux will change accordingly to satisfy equation (2.10). The variation of the stator flux changes during a short period say sampling period T_s when the stator voltage is changed is then

$$\Delta\psi_s = v_s T_s \tag{2.11}$$

Equation (2.11) shows that the stator flux space vector moves in the direction of the applied stator voltage space vector during this period. By selecting the appropriate stator voltage space vectors in subsequent time intervals, it is then possible to change the stator flux

in the desired way. Decoupled control of the stator flux and torque is achieved by acting on the radial and tangential components of the stator flux space vector. These two components are directly proportional to the components of the stator voltage space vector in the same directions as shown in **Figure.2.11**.

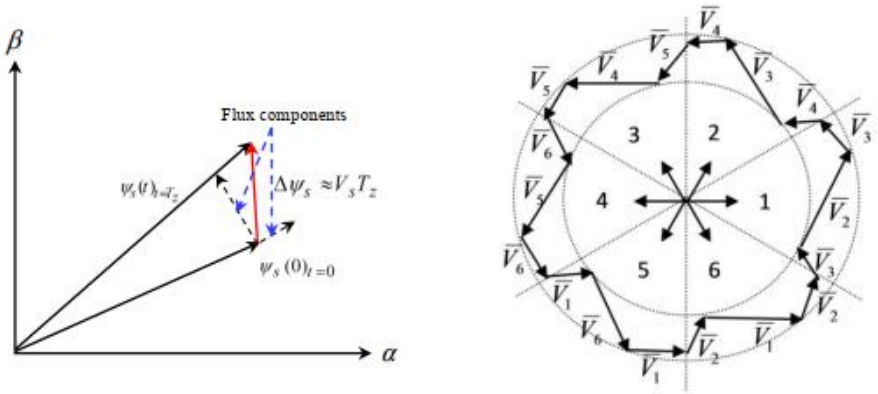

Figure.2.11 Evolution of stator flux vector in the complex plan.

A two-level hysteresis comparator is used for flux regulation. The hysteresis band keeps the flux vector extremity within the limits of the two concentric circles with close radius as shown in **Figure.2.12**.The choice of the hysteresis bandwidth h_{ψ_s} depends on the switching frequency of the inverter.

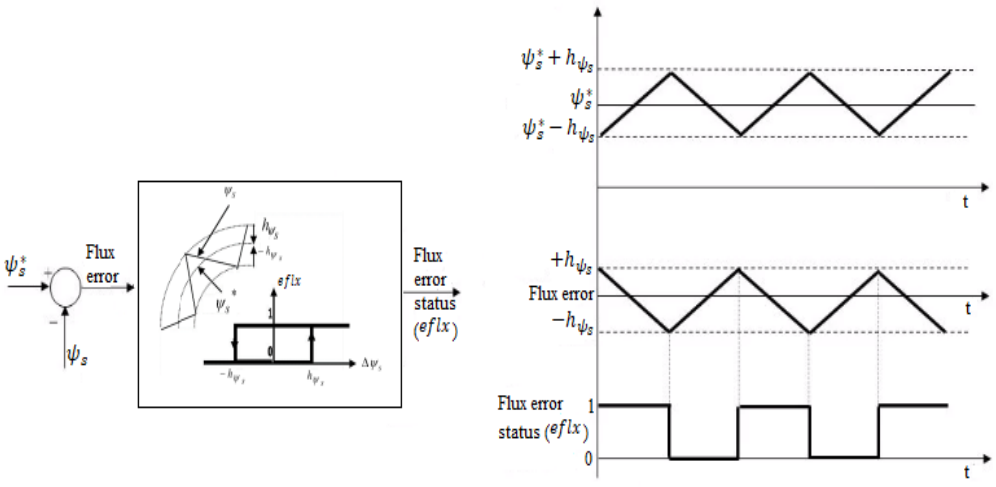

Figure.2.12 Tow-level hysteresis comparator for stator flux control**.**

The logical outputs of the flux controller are defined as:

$$\begin{cases} eflx = 1 & if\ \Delta\psi_s > h_{\psi_s} \\ eflx = 0 & if\ \Delta\psi_s \leq -h_{\psi_s} \end{cases} \quad (2.12)$$

Where $h_{\psi_s}$is the hysteresis band of stator flux and the stator flux error (*eflx*) is the difference between the reference flux value and the estimated value.

$$\Delta\psi_s = |\psi_s^*| - |\psi_s| \tag{2.13}$$

2.4.3.2. Electromagnetic torque control

Regardless of the applied method of control, the torque developed by the motor can be written as

$$\boldsymbol{T_e} = \frac{3}{2} p \frac{L_m}{\sigma L_s L_r} \psi_s \times \psi_r \tag{2.14}$$

$$T_e = \frac{3}{2} p \frac{L_m}{\sigma L_s L_r} |\psi_s||\psi_r| \sin\delta \tag{2.15}$$

Where δ is the angle between stator flux and rotor flux space vectors.

From expression (2.15), it is clear that the electromagnetic torque is controlled by the stator and rotor flux amplitudes. If those quantities are maintaining constant, the torque can be controlled by adjusting the load angle $\boldsymbol{\delta}$.

Rotor flux changes slowly because its rate of change depends on a relatively large rotor time constant; therefore, it can be assumed to be constant in a short period of time. The stator flux amplitude is also kept constant in the DTC control scheme; hence both the vectors in the equation (2.9) have constant amplitudes. Rapid change of torque can obtained if instantaneous positions of the stator flux vector are changed quickly so that δ is quickly varied, this is the essence of DTC. The instantaneous change of δ can be obtained by switching on the appropriate stator voltage space vector of the VSI as shown in **Figure.2.13**.

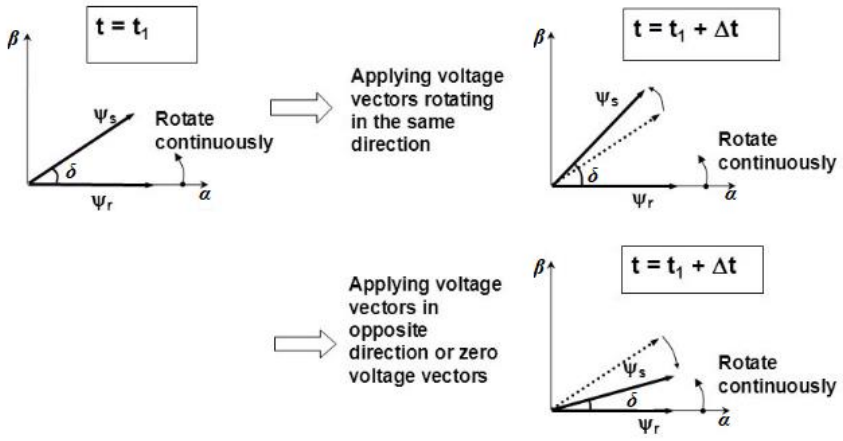

Figure.2.13 Effect of the application of different voltage vectors on the flux angle δ.

The torque regulation can be realized using three-level hysteresis comparator as shown in **Figure.2.14.** It allows motor control in both rotation senses. The tow-level comparator can be used for one rotation sense.

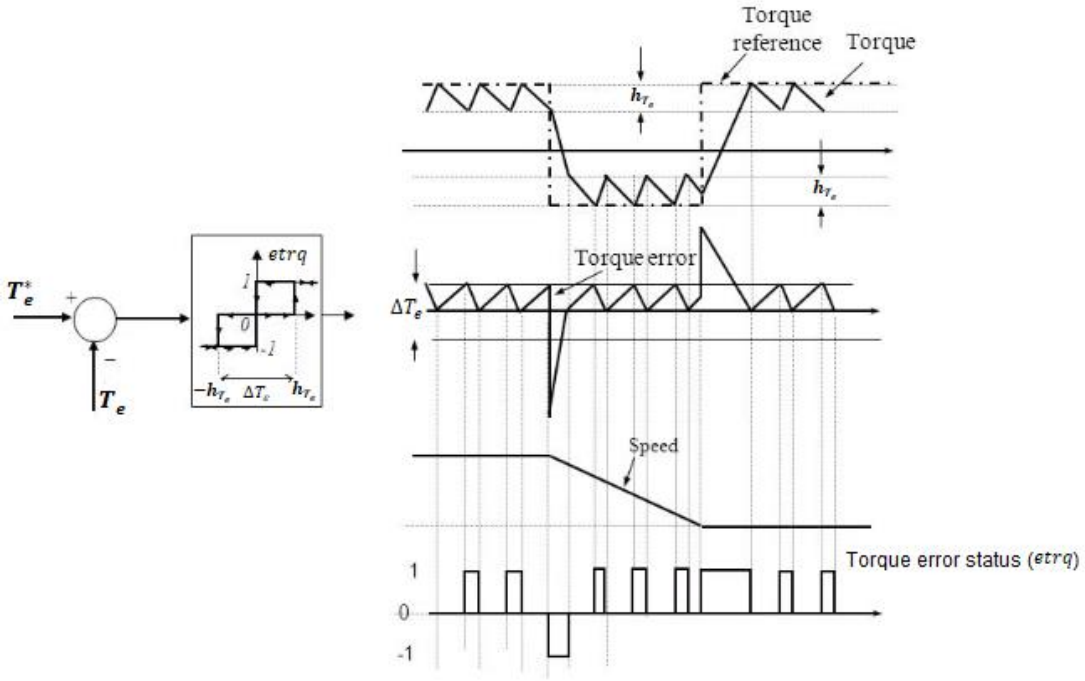

Figure.2.14 Three level hysteresis comparator for electromagnetic torque control.

The logical outputs of the torque controller are defined as:

$$\begin{cases} etrq = 1 & if\ \Delta T_e > h_{T_e} \\ etrq = 0 & if\ -h_{T_e} \le \Delta T_e \le h_{T_e} \\ etrq = -1 & if\ \Delta T_e < -h_{T_e} \end{cases} \quad (2.16)$$

Where h_{T_e} is hysteresis band of torque.

The torque error is defined by the difference between the references values of the torque and the actual estimated values:

$$\Delta T_e = T_e^* - T_e \quad (2.17)$$

2.4.4. Estimation of stator flux and electromagnetic torque

2.4.4.1. Stator flux estimation

It follows that for successful operation of a DTC scheme, it is necessary to have accurate estimates of the stator flux amplitude and the electromagnetic torque. In addition, it

is necessary to estimate in which sector of the complex plane the stator flux space vector is situated. The estimation of the stator flux is usually done by the integration of the back-emf. The stator flux components can be expressed using stator voltages and currents in the stationary reference frame (α, β) by:

$$\begin{cases} \psi_{\alpha s} = \int_0^t (v_{\alpha s} - R_s i_{\alpha s}) dt \\ \psi_{\beta s} = \int_0^t (v_{\beta s} - R_s i_{\beta s}) dt \end{cases} \quad (2.18)$$

Then, the stator flux magnitude can be obtained easily by the following expression:

$$|\psi_s| = \sqrt{\psi_{\alpha s}^2 + \psi_{\beta s}^2} \quad (2.19)$$

$$\theta_s = \tan^{-1}(\psi_{\beta s}/\psi_{\alpha s}) \quad (2.20)$$

The first step is to get the (α, β) voltage components and this is done by firstly measuring the output phase voltages and then apply the Clarke transformation as follow:

$$\begin{bmatrix} v_{\alpha s} \\ v_{\beta s} \end{bmatrix} = \begin{bmatrix} \frac{2}{3} & -\frac{1}{3} & -\frac{1}{3} \\ 0 & \frac{1}{\sqrt{3}} & -\frac{1}{\sqrt{3}} \end{bmatrix} \begin{bmatrix} v_{as} \\ v_{bs} \\ v_{cs} \end{bmatrix} \quad (2.21)$$

Where: v_{as}, v_{bs}, v_{cs} are the voltage outputs of the three-phase VSI given as:

$$\begin{cases} v_{as} = \frac{V_{dc}}{3}(2S_a - S_b - S_c) \\ v_{bs} = \frac{V_{dc}}{3}(2S_b - S_a - S_c) \\ v_{cs} = \frac{V_{dc}}{3}(2S_c - S_a - S_b) \end{cases} \quad (2.22)$$

The stator space vector current components ($i_{\alpha s}, i_{\beta s}$) can be obtained by measuring the phase currents and then apply the Clarke transformation as follow:

$$\begin{bmatrix} i_{\alpha s} \\ i_{\beta s} \end{bmatrix} = \begin{bmatrix} \frac{2}{3} & -\frac{1}{3} & -\frac{1}{3} \\ 0 & \frac{1}{\sqrt{3}} & -\frac{1}{\sqrt{3}} \end{bmatrix} \begin{bmatrix} i_{as} \\ i_{bs} \\ i_{cs} \end{bmatrix} \quad (2.23)$$

2.4.4.2. Electromagnetic torque estimation

The produced electromagnetic torque of the induction motor can be determined using the cross product of the stator quantities (i.e., stator flux and stator currents). The torque formula is expressed as following:

$$T_e = p\left(\psi_{\alpha s} i_{\beta s} - \psi_{\beta s} i_{\alpha s}\right) \quad (2.24)$$

2.4.5. Switching table and control algorithm

To maintain a decoupled control, pair of hysteresis comparators receives the stator flux and torque errors as inputs. Then, the comparators outputs determine the appropriate voltage vector selection [25; 26].

The space vectors of inverter output phase voltages are shown again in **Figure.2.15**, The sectors are all of 60 degrees and are distributed ±30 degrees around the corresponding voltage space vector, in addition the sectors are identified with Roman numeral Ⅰ to Ⅵ. If the stator flux space vector lies in the kth sector, where *k* = 1, 2, 3, 4, 5, 6, its magnitude can be increased by using the voltage vectors *k, k+1, k-1*. Its magnitude can be decreased by using *k-2, k +2*, and *k+3* vectors. However, the selected voltage vector will also affect the torque production of the induction motor. In addition, the switching frequency will also be affected. The idea is to always keep the switching frequency as low as possible so that the most appropriate voltage space vector is the one that requires the minimum number of switching and simultaneously drives both the stator flux and the torque errors in the desired direction. Which of the three possible vectors will be applied depends on the flux and torque errors.

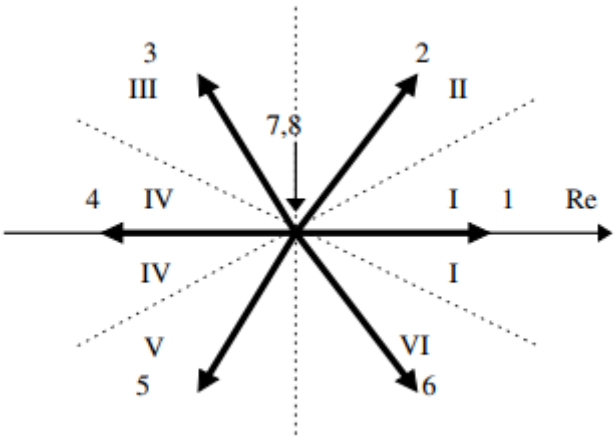

Figure .2.15 Phase voltage space vectors and appropriate sectors

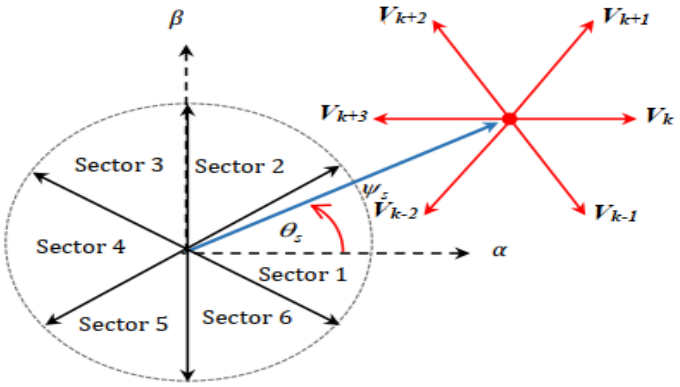

Figure.2.16 Voltage vector selection when the stator flux vector is located in sector *k*.

By the inclusion of the torque error, while the stator flux space vector is located in the sector *k* the selection of suitable voltage space vector is done as follow:

- If V_{k+1} is selected then ψ_s increases and T_e increases.
- If V_{k-1} is selected then ψ_s increases and T_e decreases.
- If V_{k+2} is selected then ψ_s decreases and T_e increases.
- If V_{k-2} is selected then ψ_s decreases and T_e decreases.

For each sector, the vectors (V_k and V_{k+3}) are not considered because both of them increase or decrease the torque in the same sector according to the position of flux vector if on the first or the second sector [27]. If the zero vectors V_0 and V_7 are selected, the stator flux will stop moving and its magnitude will not change, the electromagnetic torque will decrease slightly [28]. The resulting look-up table for DTC was proposed by Takahashi is presented in **Table.2.1**.

		Sectors					
Flux error	Torque error	I	II	III	IV	V	VI
Eflx = 1	*etrq = 1*	V_2	V_3	V_4	V_5	V_6	V_1
	etrq = 0	V_7	V_0	V_7	V_0	V_7	V_0
	etrq = -1	V_6	V_1	V_2	V_3	V_4	V_5
Eflx = 0	*etrq = 1*	V_3	V_4	V_5	V_6	V_1	V_2
	etrq = 0	V_0	V_7	V_0	V_7	V_0	V_7
	etrq = -1	V_5	V_6	V_1	V_2	V_3	V_4

Table.2.1: Optimum voltage vector look-up table.

2.5. DTC based 4 switch three-phase inverter

2.5.1. Three-phase four switch voltage source inverter

The power circuit of the IM fed from 4S3P voltage-source inverter is shown in **Figure.2.17.** This circuit is composed from two sides; the first side consists of two IGBT switches *Q1, Q2* and two capacitors *C1, C2* together constitute a single-phase half-bridge rectifier circuit, the remaining four IGBTs and the capacitor *C1, C2* together form a low cost four-switch three-phase inverter circuit. The rectifier provides the dc link voltage for the inverter and the inverter is followed by a three-phase induction motor. Phase "*a*" and phase "*b*" of the IM are connected through two limbs of the inverter, while phase "*c*" is connected to the midpoint of the capacitors bank, The maximum dc link voltage across each capacitor maintains equal to V_{dc}.

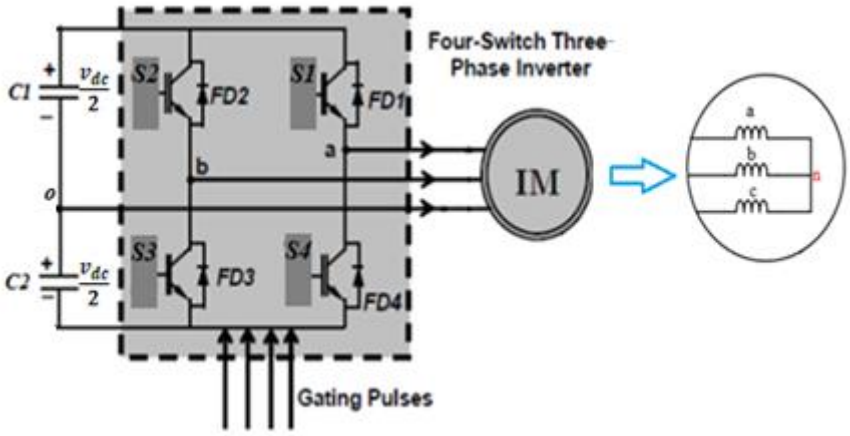

Figure.2.17 Block diagram of the IM fed by FSTP VSI

According to the scheme in Figure.2.12 the switching status of the inverter is represented by binary variables *S1* to *S4*, which are set to "1" when the switch is closed and "0" when open. In addition the switches in one inverter branch are controlled complementary (1 on, 1 off), therefore:

$$\begin{cases} S1 + S4 = 1 \\ S2 + S3 = 1 \end{cases} \quad (2.25)$$

The phase to the commun point c voltage depends on the turning off signal of the switch as in eqt (2.26) :

$$\begin{cases} V_{ao} = (2S_1 - 1)\frac{V_{dc}}{2} \\ V_{bo} = (2S_2 - 1)\frac{V_{dc}}{2} \\ V_{co} = 0 \end{cases} \quad (2.26)$$

Under balanced conditions the following equations are obtained

$$\begin{cases} v_{an} + v_{bn} + v_{cn} = 0 \\ v_{ao} + v_{bo} + v_{co} - 3v_{no} = 0 \\ v_{no} = \frac{1}{3}(v_{ao} + v_{bo} + v_{co}) \end{cases} \quad (2.27)$$

From equations 2.26 and 2.27 the phase-to-nutral voltages can be derived as follow

$$\begin{cases} v_{an} = \frac{v_{dc}}{3}(4S_1 - 2S_4 - 1) \\ v_{bn} = \frac{v_{dc}}{3}(4S_2 - 2S_3 - 1) \\ v_{cn} = -\frac{v_{dc}}{3}(S_1 + S_2 - 1) \end{cases} \quad (2.28)$$

Since there are 2 switches S_1 and S_2 that controls the output voltage, then there exists 2^2=4 possible positions of the voltage space vector from the combination of the switching states, in which all the vectors are active (V_1,V_2,V_3,V_4) and there is no zero vector [31]. The four switching states are shown as space vectors in **Figure.2.18**:

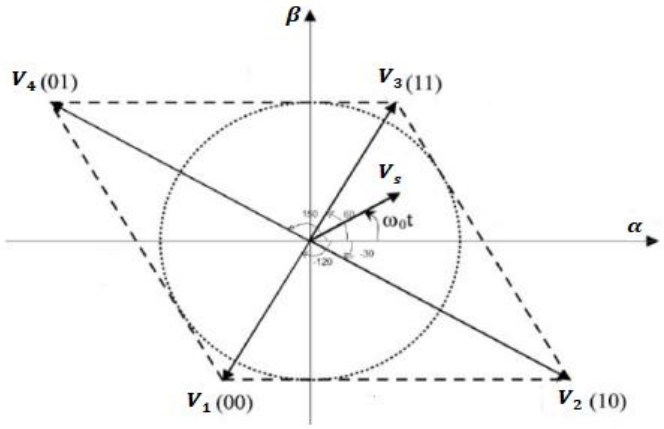

Figure.2.18 Voltage space vector of FSTPI in the αβ plan

S_1	S_2	$V_s = V_\alpha + V_\beta$
0	0	$V_1 = \frac{V_{dc}}{3} e^{-j\frac{2\pi}{3}}$
1	0	$V_2 = \frac{2V_{dc}}{3} e^{-j\frac{\pi}{6}}$
1	1	$V_3 = \frac{V_{dc}}{3} e^{j\frac{\pi}{3}}$
0	1	$V_4 = \frac{2V_{dc}}{3} e^{-j\frac{5\pi}{6}}$

Table.2.2: Combination of switching and voltage space vectors

The alpha beta plane is divided into 4 sectors 90 degree each and given as:

Sector 1	Sector 2	Sector 3	Sector 4
-30^0 $+60^0$	60^0 $+150^0$	150^0 240^0	240^0 -30^0

2.5.2. Control algorithm and switching table

The torque-flux control and estimation four FSTPI are done exactly the same way as the SSTPI.

The objective of the DTC is to keep the motor torque and stator flux within a defined band of tolerance by selecting the most convenient voltage space vector from (switching table). In the case of the conventional switching table of DTC for FSTPI-IM, one of four active vectors is chosen (Table 2.3) [30].

Flux error	Torque error	Sector 1	Sector 2	Sector 3	Sector 4
1	1	V_1	V_2	V_3	V_4
1	-1	V_4	V_1	V_2	V_3
0	1	V_2	V_3	V_4	V_1
0	-1	V_3	V_4	V_1	V_2

Table 2.3: Conventional switching table for DTC control method

2.5.3. Improved Switching Technique for DTC

In order to reduce the torque and speed ripples by using the principle of similarity for voltage space vectors, an optimized vector selection table corresponding to the introduced DTC strategy of FSTPI is originally established for induction machine in 2013 [31] similarly to the basic SSTPI switching table. The αβ plan is divided in to six sectors, and for each sector, the optimal space vector is chosen accordingly to the required torque and flux by using the effective vectors (**equations 2.29, 2.30** and **Figure.2.19**). These vectors are synthesized using the basic space vectors with the duty cycle of 50% (switching period is *Ts*). The same way is done for effective zero space vector (**Table.2.5**).

To simulate six non-zero vectors in SSTPI, beside the two V_1 and V_3, it can be used then effective vectors V_{23M}, V_{43M}, V_{14M} and V_{12M}. These vectors are formed as follows:

$$\begin{cases} V_{23M} = \frac{1}{2}(V_2 + V_3) = \frac{V_{dc}}{3} e^{j0} \\ V_{43M} = \frac{1}{2}(V_4 + V_3) = \frac{V_{dc}}{3} e^{j\frac{2\pi}{3}} \\ V_{14M} = \frac{1}{2}(V_1 + V_4) = \frac{V_{dc}}{3} e^{j\pi} \\ V_{12M} = \frac{1}{2}(V_1 + V_2) = \frac{V_{dc}}{3} e^{-j\frac{2\pi}{3}} \end{cases} \quad (2.29)$$

The zero vectors V_7 and V_0 can be represented by the vector V_{0M} which can be simulated as follow:

$$V_{0M} = \frac{1}{2}(V_1 + V_3) \quad (2.30)$$

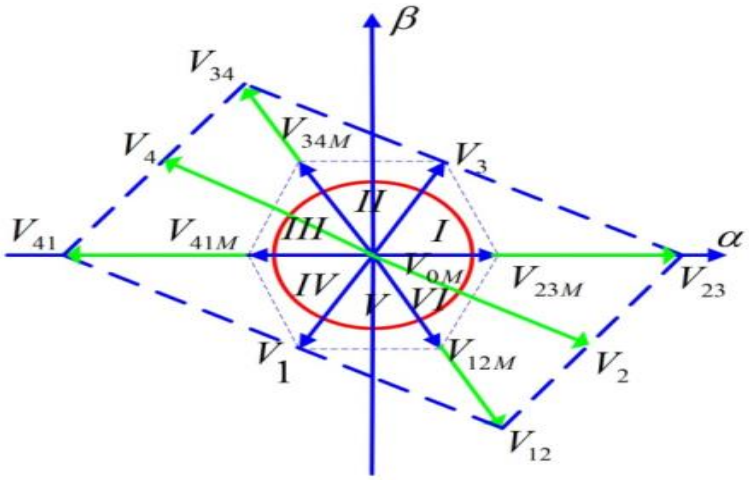

Figure.2.19 Voltage space vectors for (FSTPI) on the principle of similarity

Used voltage space vectors for **SSTPI**	Used voltage space vectors for **FSTPI**
V_1	V_{23M}
V_2	V_3
V_3	V_{43M}
V_4	V_{14M}
V_5	V_1
V_6	V_{12M}
V_0, V_7	V_{0M}

Table.2.4: Similarity between space vectors of FSTPI and SSTPI

The lookup table is constructed using the same principle as the SS DTC and it is given in **Table.2.5** below:

Flux Error	Torque Error	Sectors					
		Ⅰ $+30^0$-30^0	**Ⅱ** 30^0 $+90^0$	**Ⅲ** 90^0 $+150^0$	**Ⅳ** 150^0+210^0	**Ⅴ** 210^0+270^0	**Ⅵ** 270^0+330^0
1	1	V_3	V_{43M}	V_{14M}	V_1	V_{12M}	V_{23M}
	-1	V_{12M}	V_{23M}	V_3	V_{43M}	V_{14M}	V_1
	0	V_{13M}	V_{13M}	V_{13M}	V_{13M}	V_{13M}	V_{13M}
-1	1	V_{43M}	V_{14M}	V_1	V_{12M}	V_{23M}	V_3
	-1	V_1	V_{12M}	V_{23M}	V_3	V_{43M}	V_{14M}
	0	V_{13M}	V_{13M}	V_{13M}	V_{13M}	V_{13M}	V_{13M}

Table.2.5 Modified switching table for DTC control method based FSTPI

2.6. Speed regulation in DTC strategy

For many industrial applications DTC can be classified as speed sensorless strategy, since it has the ability to operate even without a speed regulation loop, which in turn doesn't require any knowledge about rotor speed. Otherwise, to achieve an adjustable speed control it is necessary to employ a speed controller for speed regulation and generation of the electromagnetic torque.

Commonly, a proportional integrator (PI) controller is employed for the regulation. It is achieved by direct comparison of the reference speed and the actual measured one than an error signal is generated (speed error) and fed to the PI controller, by correctly adjusting the controller gains the reference torque is then generated. The poles placement method is used to determine the controller gains (Appendix A.2).

2.7. Control scheme of basic DTC

The basic control scheme of basic DTC is shown in **Figure.2.20**. It consists of speed regulation loop using PI controller, decoupled flux and torque hysteresis controllers, look-up switching table, an association of VSI-Induction motor, voltage and current calculation blocks with the Park transformation and flux/torque estimators with position/sector determination.

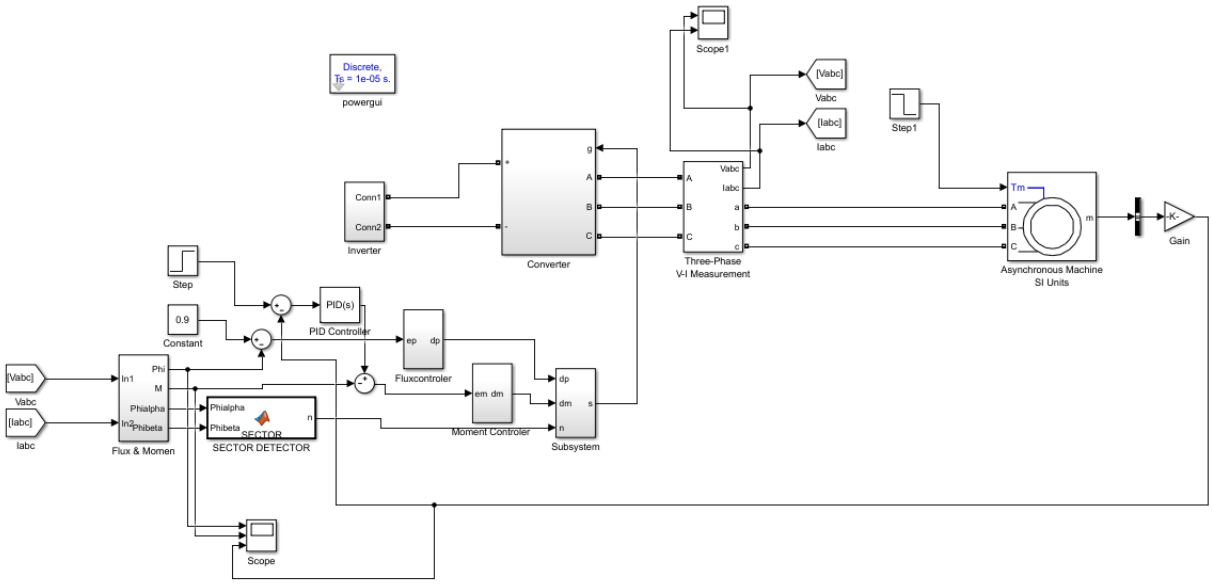

Figure.2.20 The basic control scheme of DTC strategy

2.8. Conclusion

Direct torque control for motor drive applications has been well established. It offers a simple control structure, fast response, and robust operation in four quadrants. The number of power switches used can be minimized using four switch inverter instead of a classical 6 switch inverter with an enhanced algorithm that gives a good performance results.

CHAPTER 3

SIMULATION AND RESULTS

3.1. Introduction

In this chapter the DTC control algorithms have been simulated by MATLAB/Simulink software. The two switch PWM rectifier is investigated and simulated for different modes of operation. A comparative study between the switching table DTC using SSTPI, DTC using FSTPI and DTC using the improved FSTPI is presented.

3.2. Simulation parameters

The simulation has been conducted for a three phases *2 kW* squirrel-cage induction motor with characteristics given in the appendix (A.II). Different operation conditions are employed for the three control method under different mode of operations. For the classical DTC, the chosen bandwidths of the hysteresis controllers are ± *0.005Wb* for flux and ±*0. 5 N.m* for the torque. The peak input voltage of the rectifier is set to $230\sqrt{2}$ V as shown in **Figure.3.1**, and the reference output voltage V_0 is set to twice Vs + 15% margine to insure a full control on the rectifier (V_0 = 750 V). The sampling period is set to 10 μs .

The speed ,torque and flux settings are shown in **Table.3.1** below:

Time [Sec]	0 – 0.5	0.5 - 1	1 – 1.5	1.5 – 2.5	2.5 – 3
Speed [Rpm]	+ 1000			−1000	
Torque[N.M]	0	+ 10	−10		+ 10
Flux [Wb]	0.9				

Table.3.1 Speed and totque settings

3.3. Rectifier simulation and results

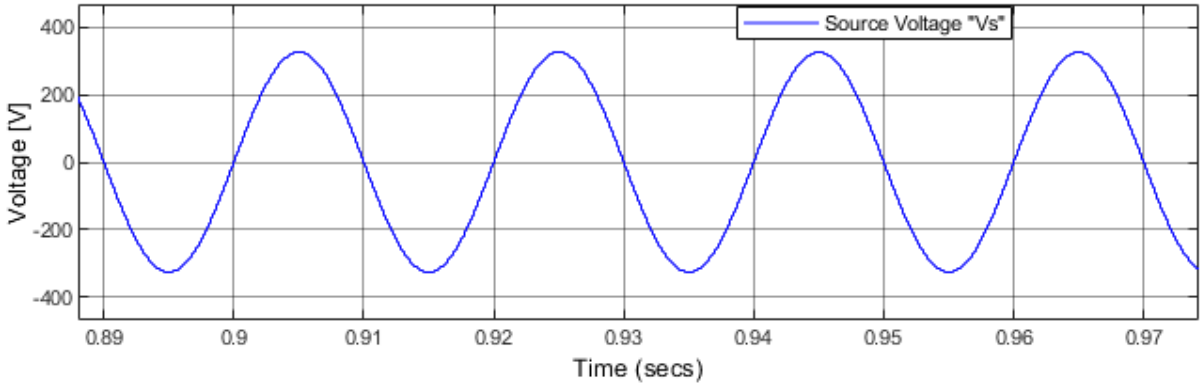

Figure.3.1 Source voltage (input voltage) applied to the boost rectifier.

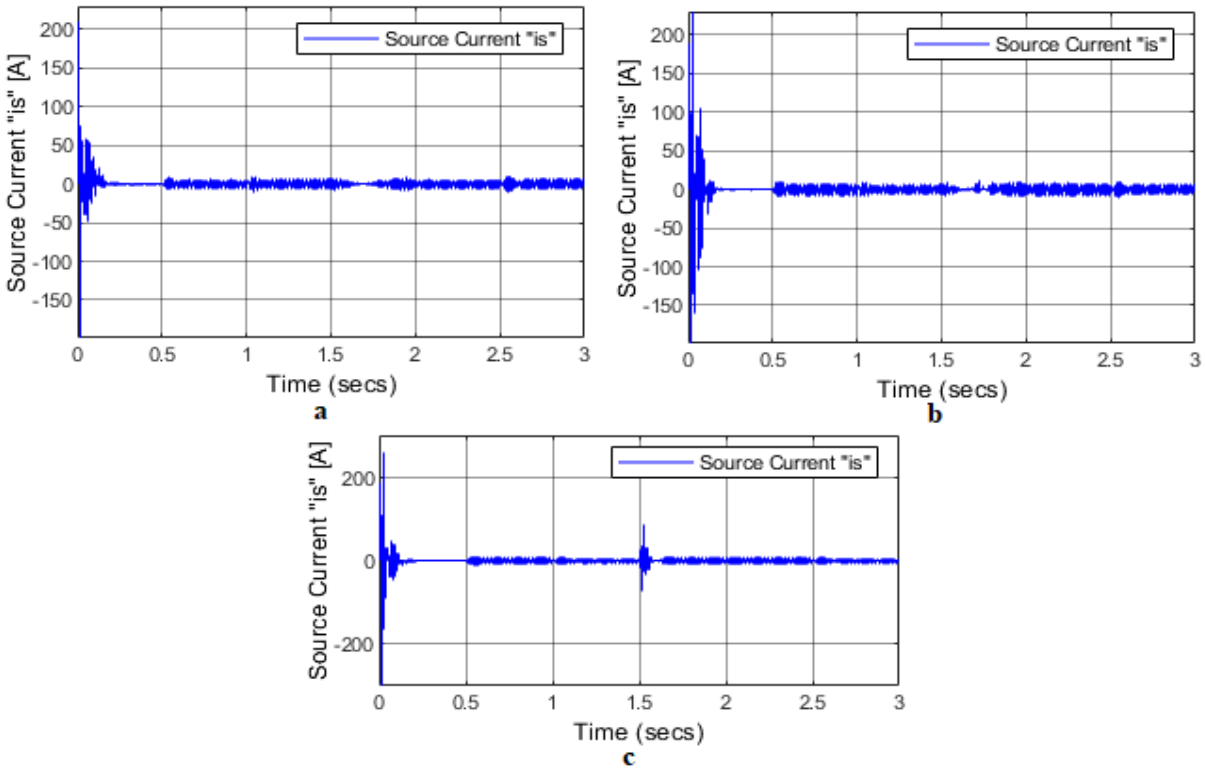

Figure.3.2 Source current of the PWM rectifier (a: SSTPI, b: FSTPI, c: improved FSTPI)

Figure.3.2 gives the input current of the rectifier behavior under the four modes of operation.

Note: the input current is multiplied by a gain of 30.

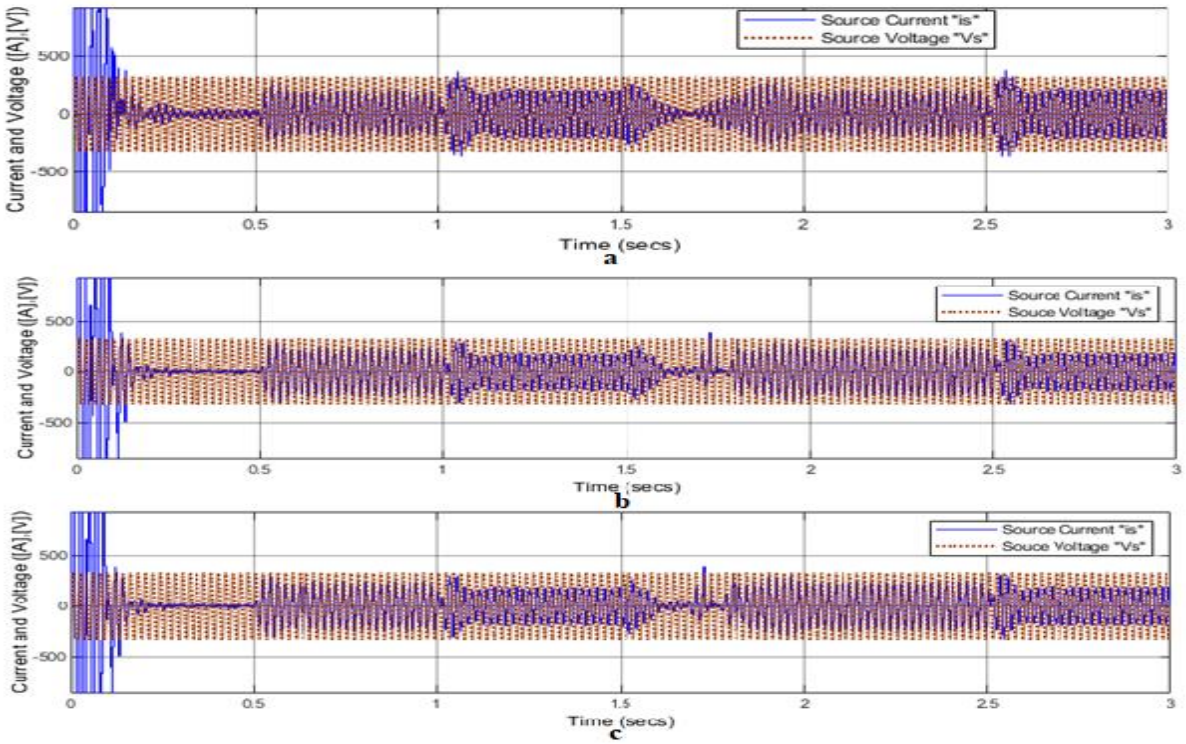

Figure.3.3 Source voltage and current drawn by the PWM rectifier (a: SSTPI, b: FSTPI, c: improved FSTPI)

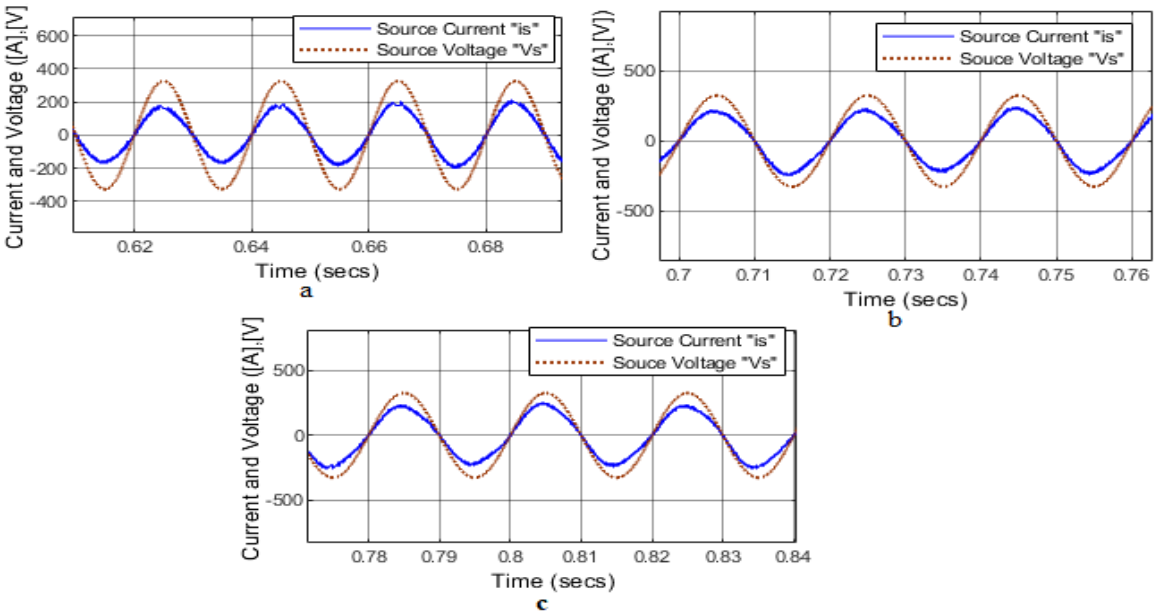

Figure.3.4 ZOOM of source voltage and current of the PWM rectifier working in the **first quadrant** (Sp+, Te) (a: SSTPI, b: FSTPI, c: improved FSTPI)

Figure.3.4 shows the behavior of the source current from t = 0.5 to 1 [sec]; a torque of 10 [N.M] is applied with a positive speed (1st Q) so; the system draws power from the source (motoring mode).

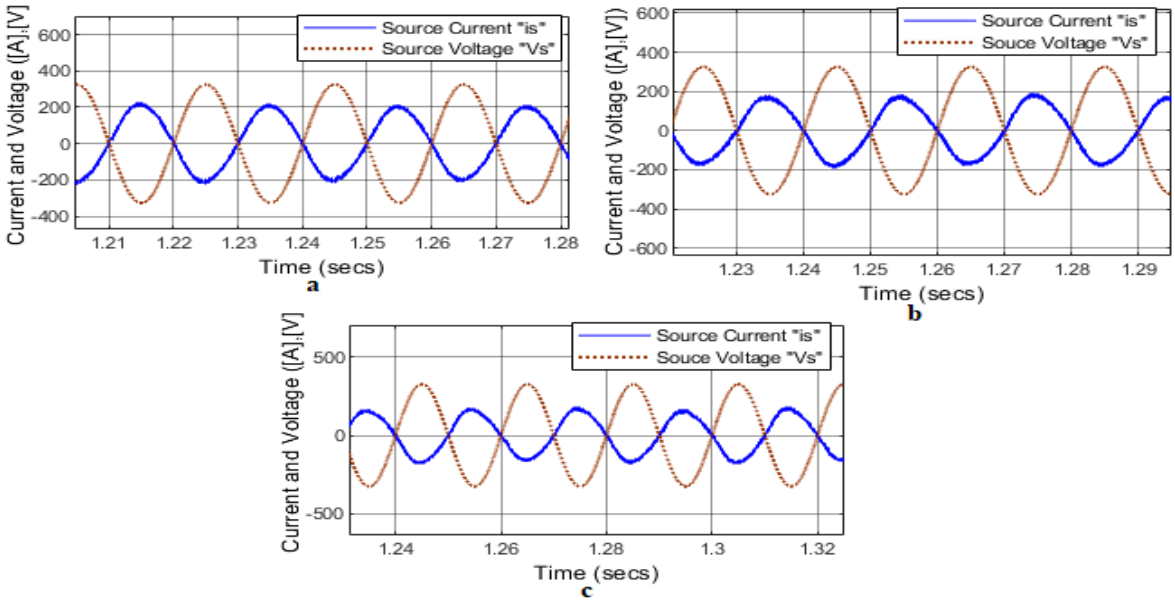

Figure.3.5 ZOOM of source voltage and current of the PWM rectifier working in the **second quadran**t (Sp-, Te+) (a: SSTPI, b: FSTPI, c: improved FSTPI)

Figure.3.5 shows the behavior of the source current from t = 1 to 1.5 [sec] sec where a reverse torque is applied while the speed is positive (2nd Q); the rectifier current in this case is 180 degree phase shifted with the source voltage hence the system is working as a generator and delivers power to the source (forward regenerating (braking)).

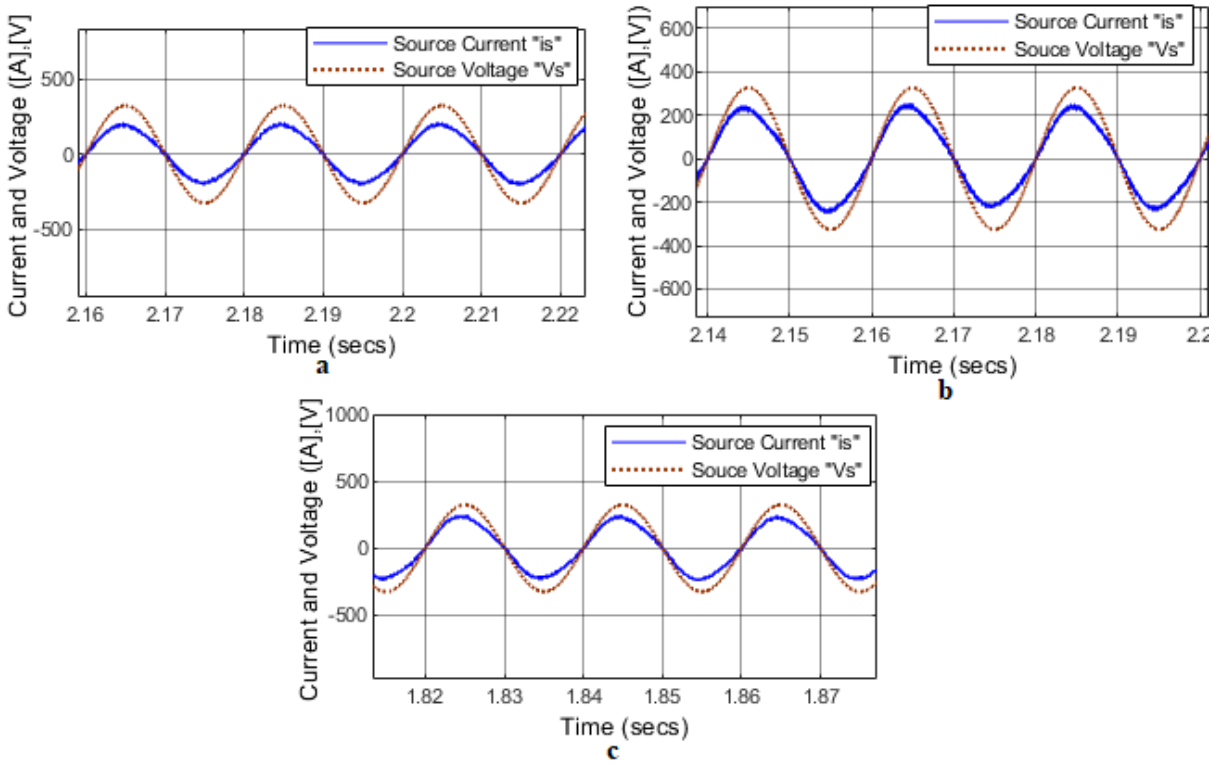

Figure.3.6 ZOOM of source voltage and current of the PWM rectifier working in the **third quadran**t (Sp-, Te-) (a: SSTPI, b: FSTPI, c: improved FSTPI)

In **Figure.3.6** from t = 1.5 to 2.5 [sec] the torque and the speed are both negative (3rd Q); in this situation the voltage and current of the source are in phase and the power is positive from the source to the motor, hence the system is working in reverse motoring mode.

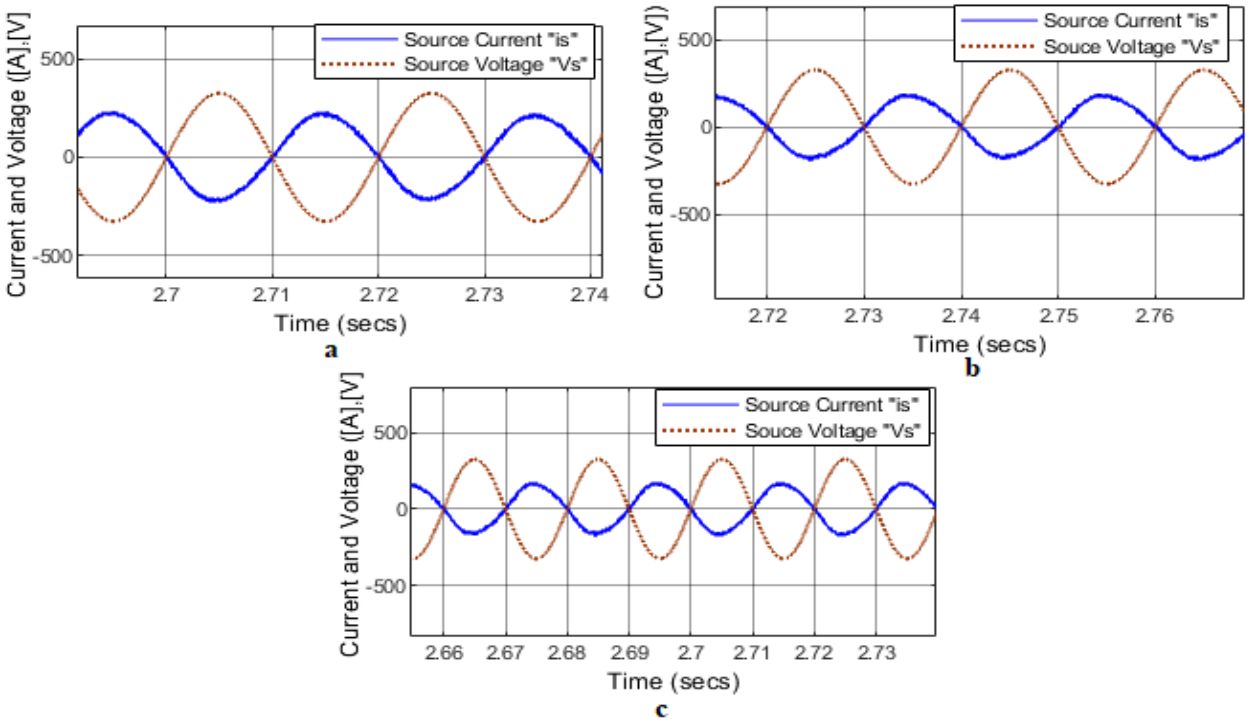

Figure.3.7 ZOOM of source voltage and current of the PWM rectifier working in the **fourth quadran**t (Sp-, Te+) (a: SSTPI, b: FSTPI, c: improved FSTPI)

Figure.3.7 gives the result of subjecting the system to a positive torque while the speed is negative (from t = 2.5 to 3 [sec]) (4^{th} Q operation); this condition leads to a phase shift of 180 degree between the source voltage and current that is the current is reversed and flow from the motor to the source (reverse regenerating (braking)) and obviously the power direction changes to negative.

Figure.3.3 to 3.7 shows that the power factor is high and close to ± 1 (phase shift ≈ 0).

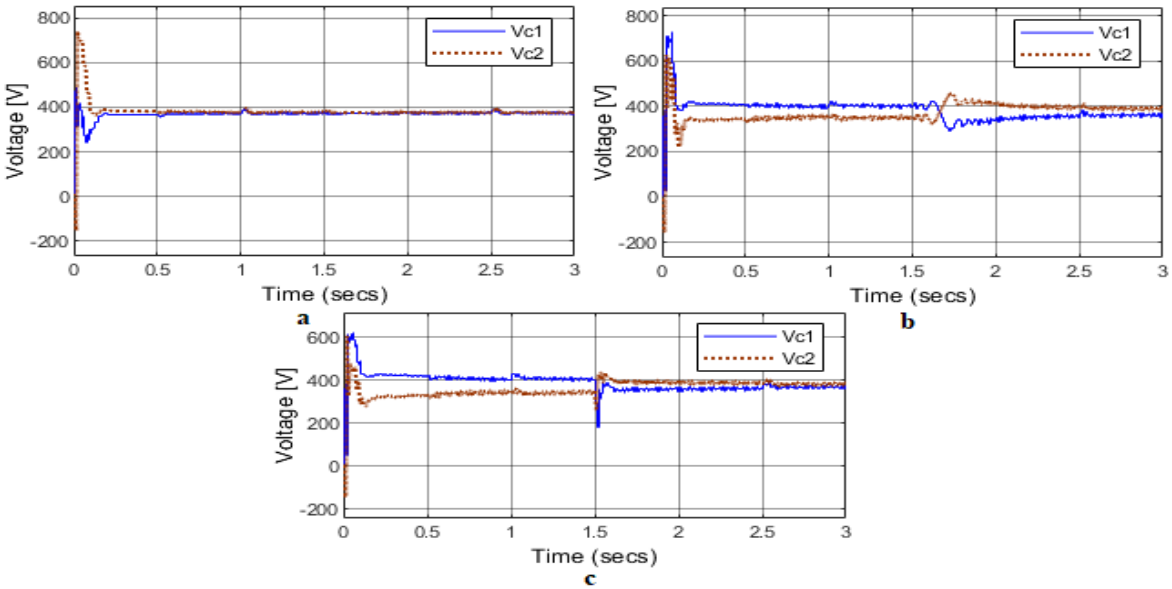

Figure.3.8 Capacitor voltages (a: SSTPI, b: FSTPI, c: improved FSTPI)

Figure3.8 gives the capacitor voltages, it is clear that for SSTFI DTC the voltages reaches the steady state very quick whereas, in FSTPI takes more time.

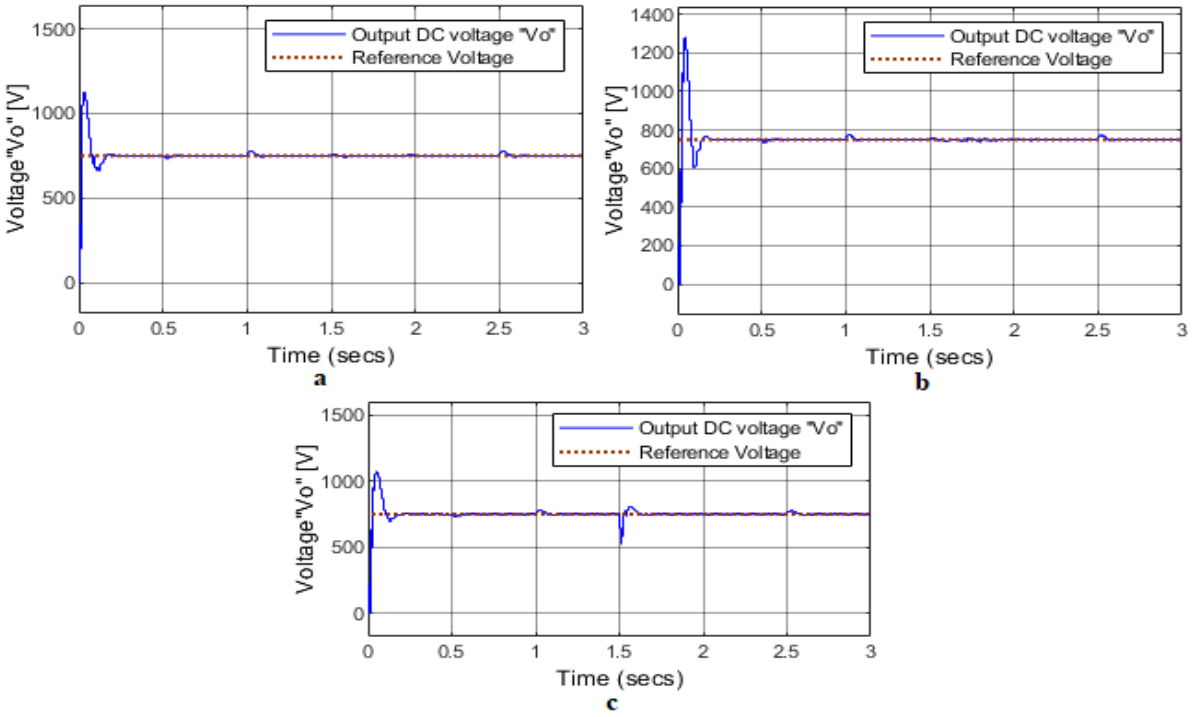

Figure.3.9 Output voltage of the PWM rectifier (a: SSTPI, b: FSTPI, c: improved FSTPI)

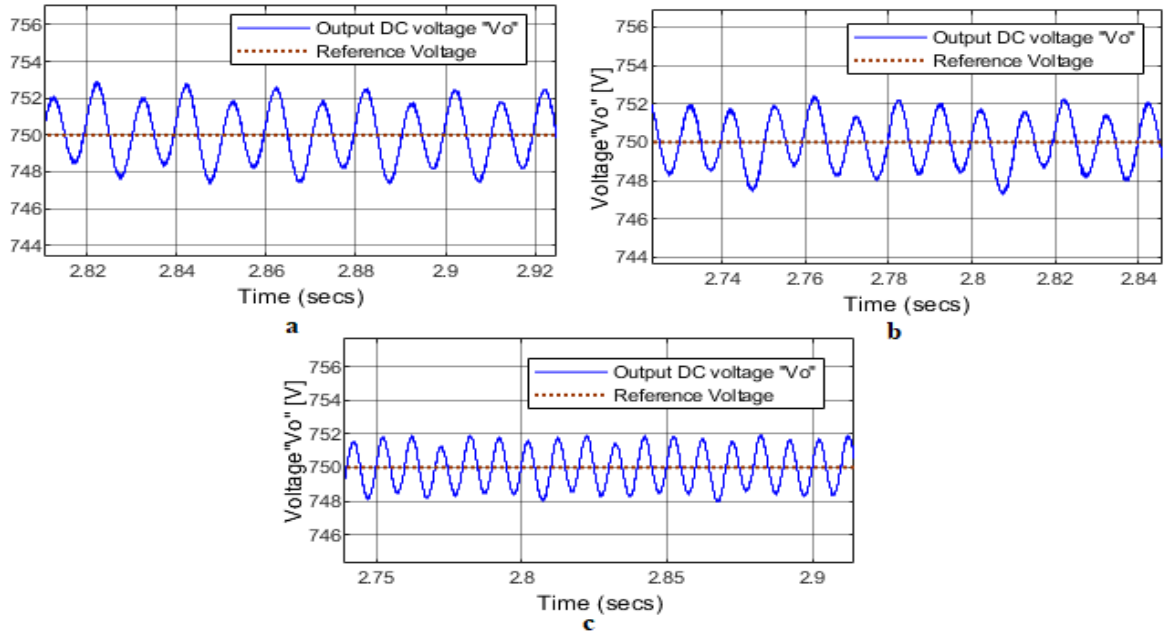

Figure.3.10 ZOOM of output voltage of the PWM rectifier (a: SSTPI, b: FSTPI, c: improved FSTPI)

Figure.3.9 and **3.10** shows the terminal output voltage for each control method, as it can be seen they almost have the same output.

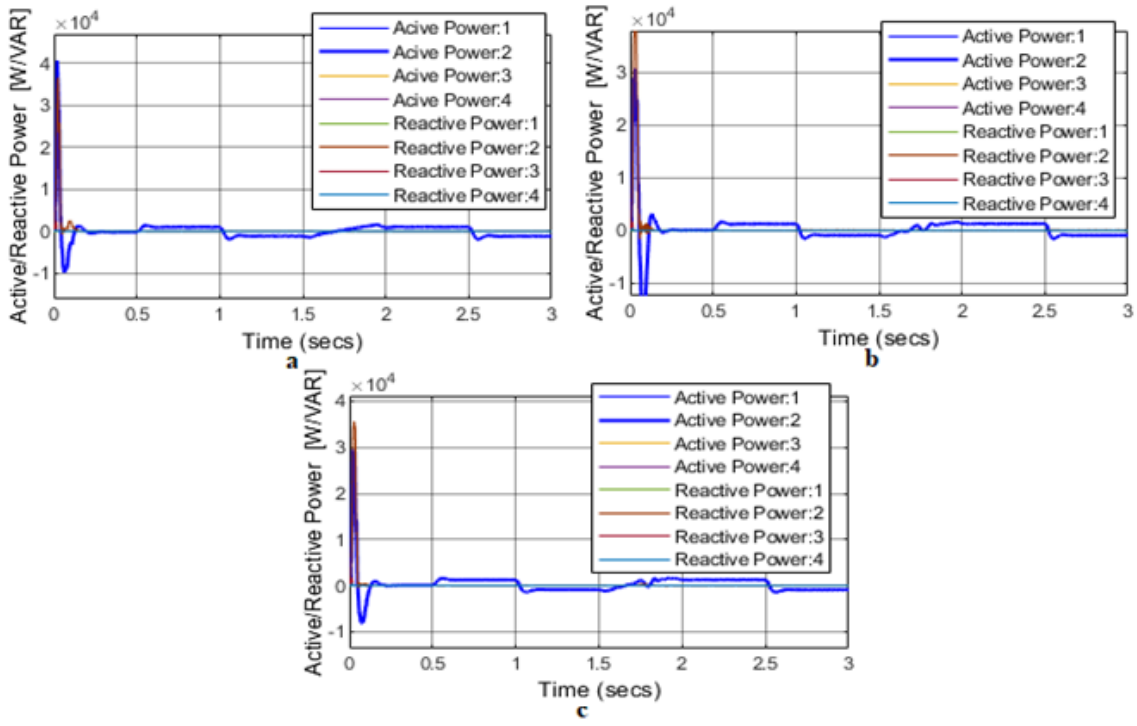

Figure.3.11 Active and reactive power drawn from the PWM rectifier during the four mode of operation (a: SSTPI, b: FSTPI, c: improved FSTPI)

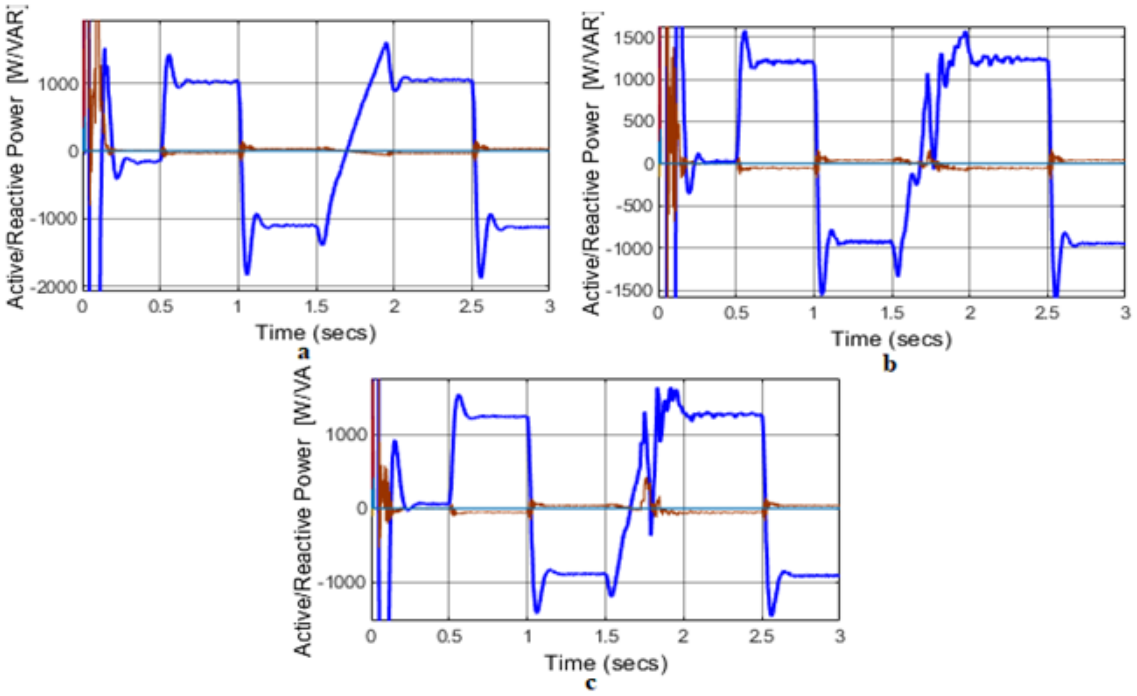

Figure.3.12 ZOOM of active and reactive power drawn from the PWM rectifier during the four mode of operation (a: SSTPI, b: FSTPI, c: improved FSTPI)

Figure.3.12 gives the power flow during the four operating modes; from t = 0.5 to 1 [sec] and from t = 1.5 to t = 2.5 the rectifier delevers power to the load (1st Q, 3rd Q), from t = 1 to 1.5 [sec] and from t = 2.5 to t = 3 [sec] the rectifier receives power from the load (2nd Q, 4th Q).

The power factor of the rectifier can be calculated from the power curve as follow:

$$Pf = \frac{P}{S} \tag{3.1}$$

- As an example the graph b of Figure.3.12 (a) at t= 0.5 to 1 [sec].

P = 1020 [W], Q = -27 [Var] hence S = 1020.36 VA
Pf = 0.9996.

3.2. Inverter simulation and results

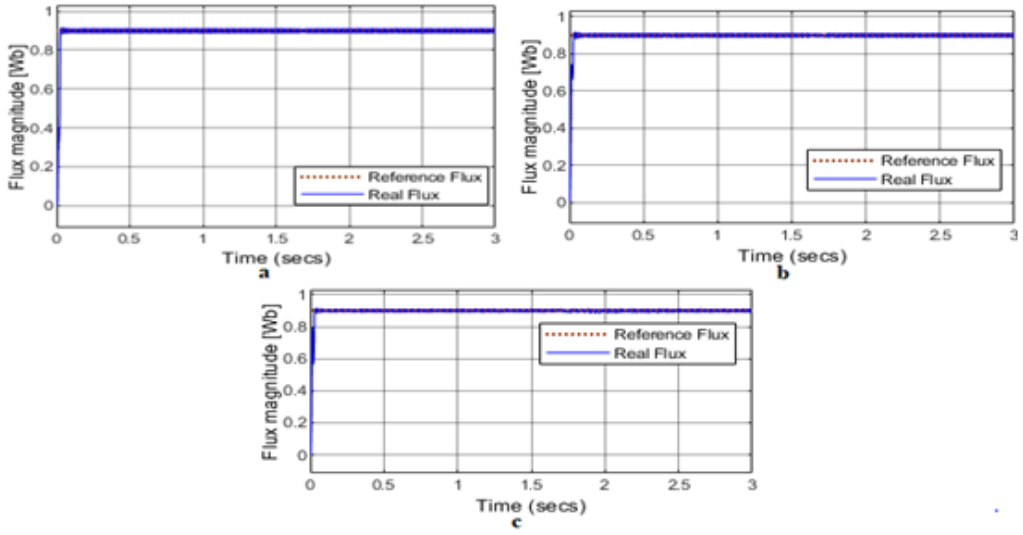

Figure.3.13 Stator flux magnitude (a: SSTPI, b: FSTPI, c: improved FSTPI)

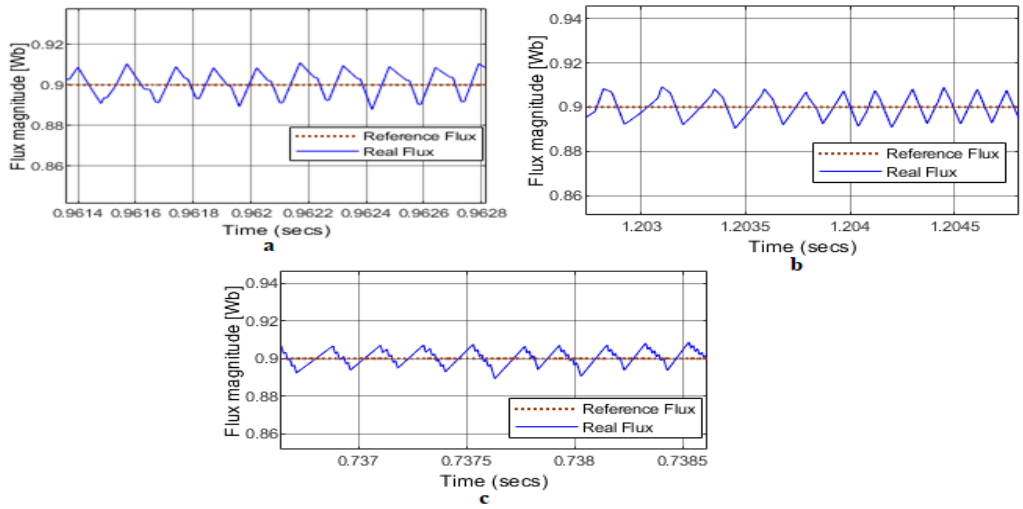

Figure.3.14 Zoom of stator flux magnitude (a: SSTPI, b: FSTPI, c: improved FSTPI)

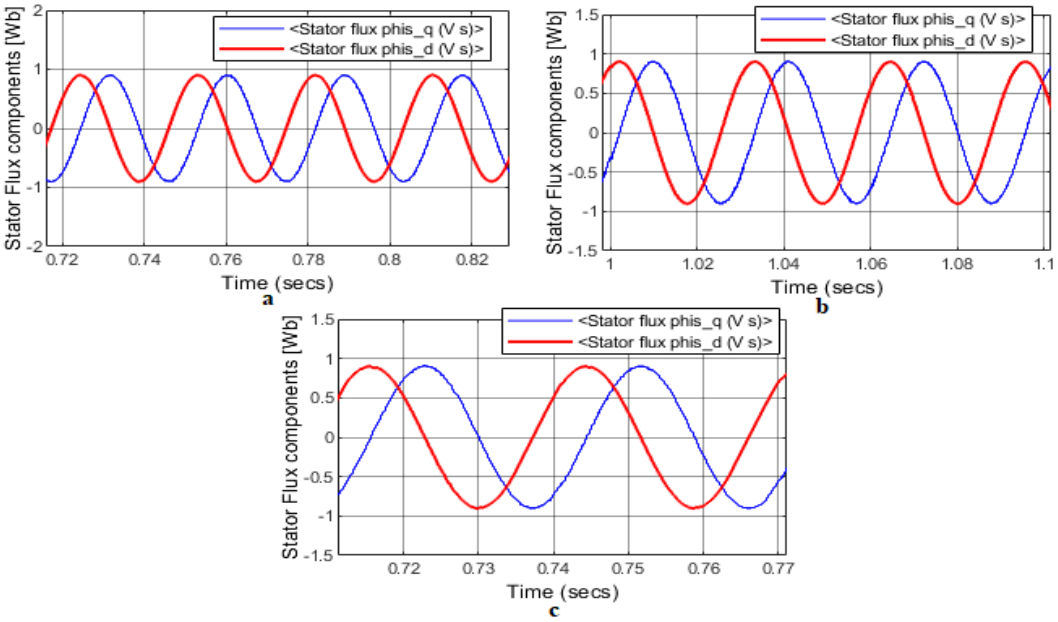

Figure.3.15 ZOOM of stator flux components (a: SSTPI, b: FSTPI, c: improved FSTPI)

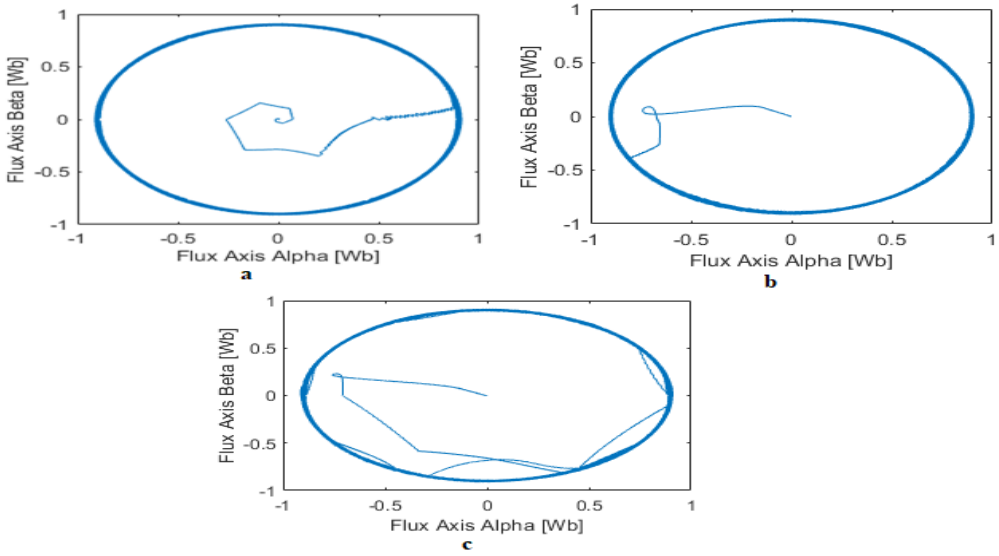

Figure.3.16 Flux circular trajectory (α,β) (a: SSTPI, b: FSTPI, c: improved FSTPI)

Figures **3.13** untill **3.16** shows flux reponse of DTC using SSTPI, FSTPI and improved FSTPI, from the figures the flux regulation is very good for all methods with a bandwidth is ± 0.05 [Wb].

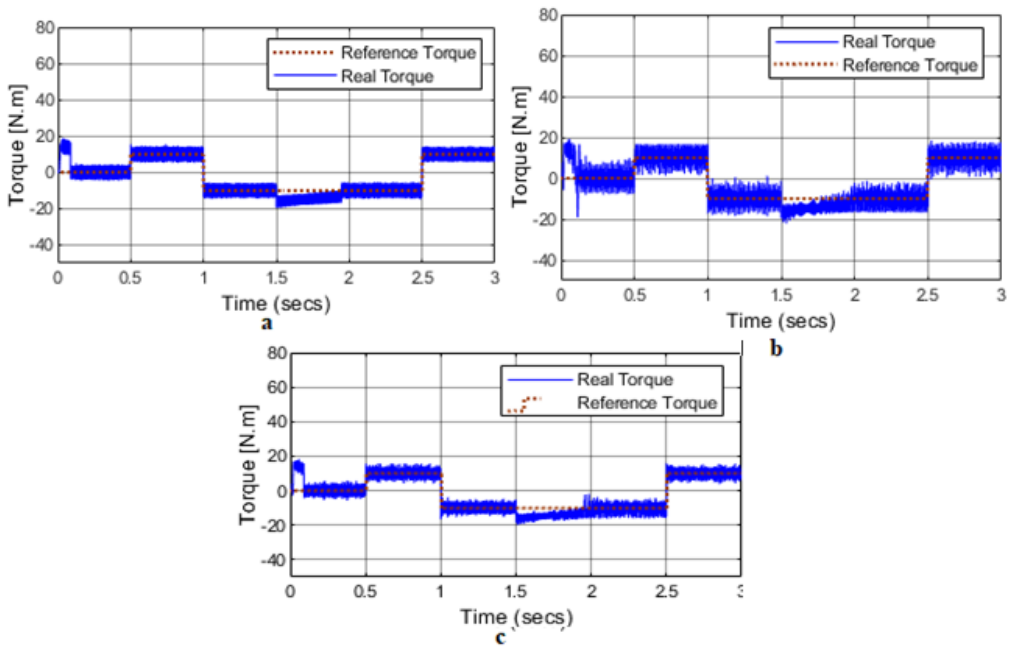

Figure.3.17 Torque response (a: SSTPI, b: FSTPI, c: improved FSTPI)

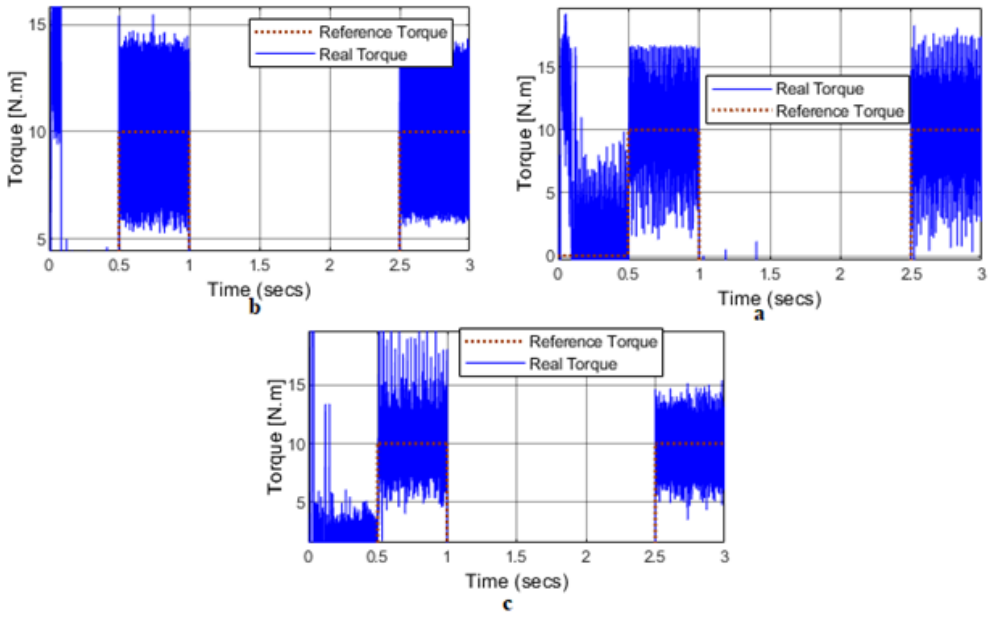

Figure.3.18 ZOOM of torque response (a: SSTPI, b: FSTPI, c: improved FSTPI)

Figures 3.17 and **3.18** gives the torque response; it is very clear that the DTC based SSTPI gives better result than any other method with hysterisis band of ± 3.5 [N.m], followed by the basic FSTPI with hysterises band of ± 5 [N.m], and finaly the inhanced FS with ± 4 [N.m] this can be improved by increasing the sampling frequency and hysterises band settings .

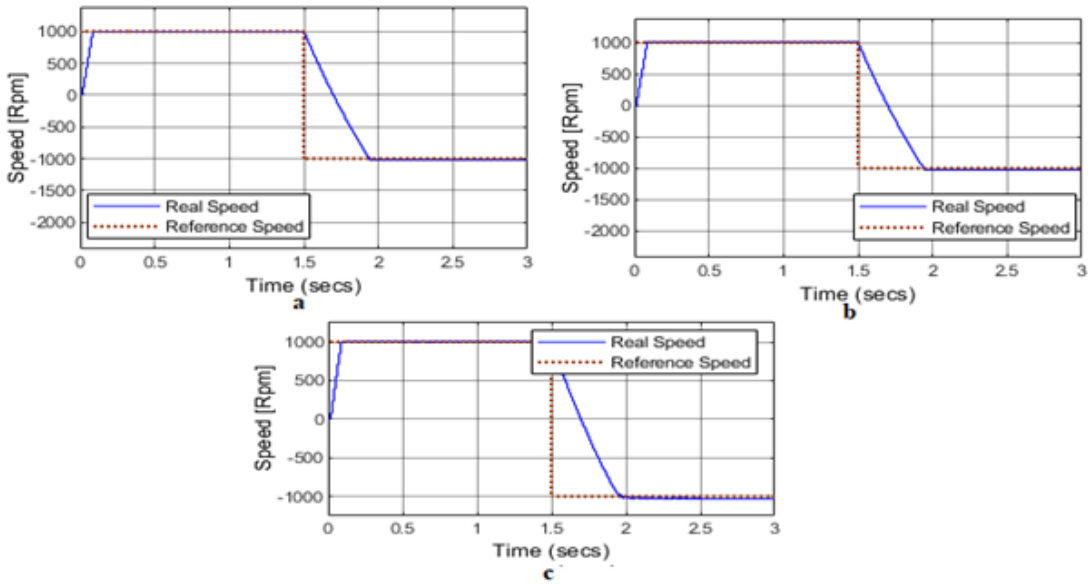

Figure.3.19 Rotor speed response (a: SSTPI, b: FSTPI, c: improved FSTPI)

Figure 3.19 shows the speed response it is clear that the speed regulation at steady state is good for the three methods under all load conditions, for the transient state it can be improved by a good selection of the speed controller.

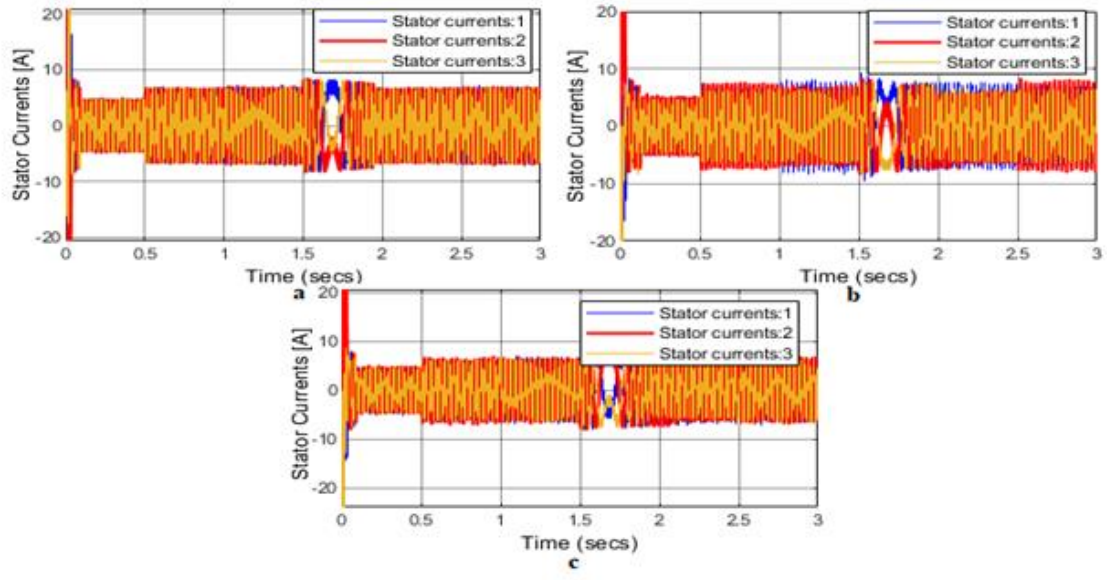

Figure.3.20 Stator currents(a: SSTPI, b: FSTPI, c: improved FSTPI)

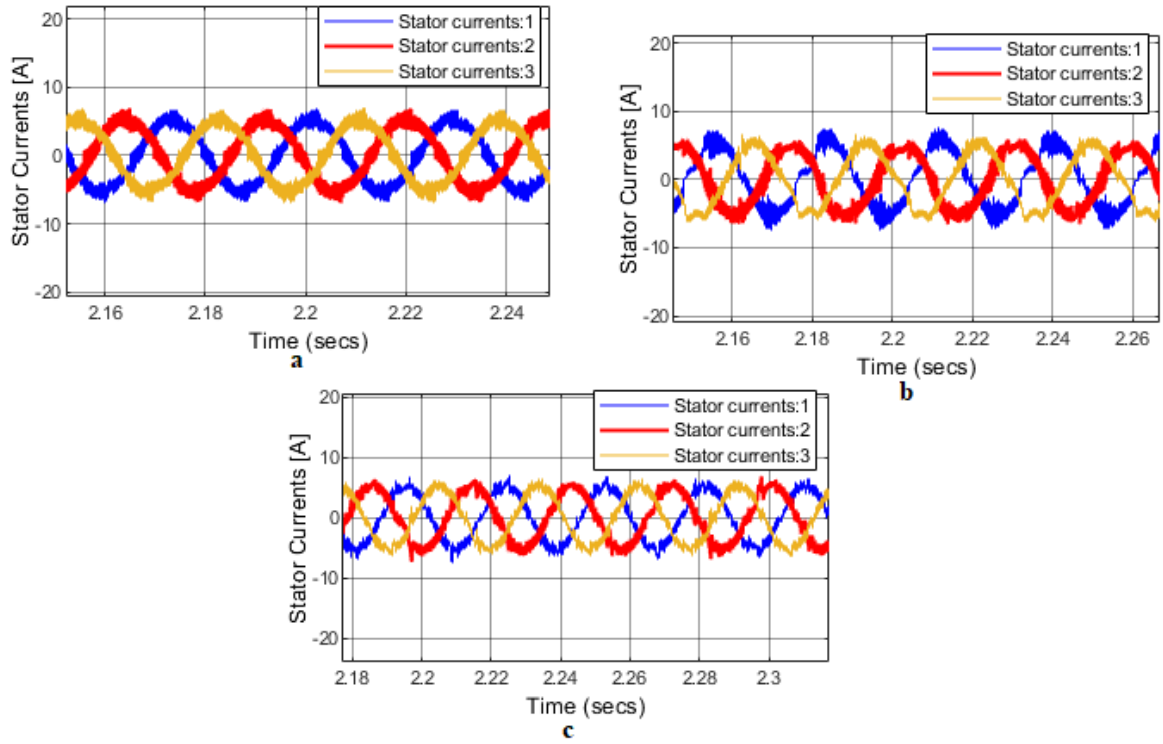

Figure.3.21 ZOOM of stator currents (a: SSTPI, b: FSTPI, c: improved FSTPI)

Finaly the motor stator currents are shown in **Figures.3.20** and **3.21**; the curents are almost, a good results where obtained for DTC based SSTPI and enhance FSTPI sinusoidal with 120 degree phase shift.

The comparaison between the different methods can be summerized in **Table.3.2** below:

	Flux	**Torque**	**Speed**
DTC based SSTPI	Very good	Medium	Good
DTC based FSTPI	Good	Poor	Good
Enhanced FSTPI DTC	Very good	Midium	Good

Table.3.2: Comparaison summary between the three investigated methods

3.3 Conclusion:

Table.3.2 summarizes the performance of the three methods, the speed and flux responses are good whereas, the torque response of basic FSTPI DTC is poor, and this last can be improved using the enhanced FSTPI DTC technique.

General conclusion

In this work, we have presented the bidirectional DTC of the Induction machine using a reduced number of power switches. The latter is considered as an alternative to the field oriented control which has the major drawback of being relatively sensitive to variations in machine parameters. On the other hand, DTC, is also simple, interesting considering its simplicity; in particular, by the fact that it does need neither real-time speed measurement, nor complex control by modulation of pulse width (PWM) of the inverter. Its calculation algorithm is simple since it is linked to a machine model where the only parameter involved is the stator resistance. In addition, the PWM is replaced in this command by a simple switching table. Of plus a very significant improvement in the performance of classic DTC has been achieved following the use of several approaches aimed at minimizing the of the torque ripples.

This work was a successful debut experience in the direct torque control of the induction machine control. The work dealt with a new DTC strategy dedicated to four-switch three phase inverter Induction Machine drives powered by two switch PWM rectifier.

An effectively caparison between SSTPI and FSTPI performance has been done. The simulation result as it was expected shows the high torque ripple introduced in the FSTPI model comparing the SSTPI model. We aimed in this work to set a DTC strategy to improve the performance of the FSTPI . The proposed DTC strategy is based on the emulation of the operation of a conventional six-switch three phase inverter SSTPI. This has been achieved thanks to suitable combinations of the four unbalanced voltage vectors intrinsically generated by the FSTPI, leading to the synthesis of the six balanced voltage vectors yielded by the SSTPI. This approach has been adopted in the design of the vector selection table which is simply addressed by hysteresis controllers, considering a subdivision of the Clarke plane into six sectors.

The simulation result shows successful improvement of the performance of the four switch inverter. In this context, the work has been addressed the reduction of high ripples and

harmonics level which is caused by the reduction of the number of switches in the four-switch inverter.

Finally, we recommend further research on the order by DTC, where several improvements can be made to this work, namely:

- Real time experimental implementation of FSTPI DTC
- The use of multi-level inverters and matrix converters to increase the number of useful voltage vectors, which minimizes fluctuations in the electromagnetic torque.
- The use of a robust observer / estimator allowing the estimation of the speed rotor as artificial intelligence techniques.

Appendix

A.1. Mathematical Modeling Of Induction Motor

A.1.1. Induction Motor Description

A dynamic model of the machine subjected to control must be known in order to understand and design of vector controlled drives. Due to the fact that every good control has to face any possible change of the plant, it could be said that the dynamic model of the machine could be just a good approximation of the real plant. Nevertheless, the model should incorporate all the important dynamic effects occurring during both steady state and transient operations. Furthermore, it should be valid for any changes in the inverters supply such as voltages or currents. Such a model can be obtained by means of either the space vector phasor theory or two-axis theory of electrical machines. The cross section of three phase squirrel cage induction motor is shown in **Figure.A.1.**

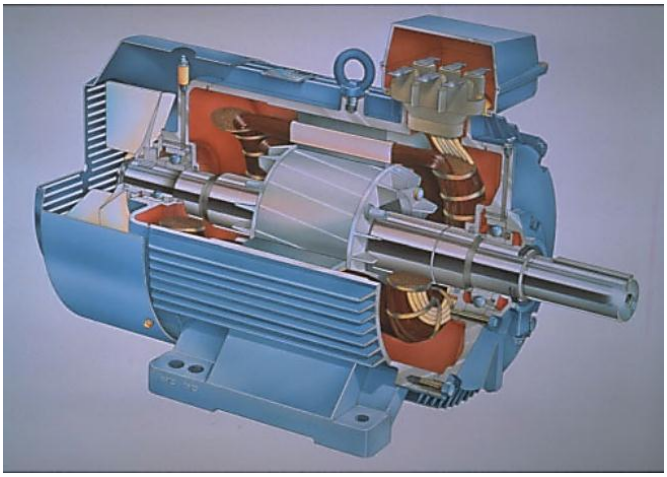

Figure.A.1 Cross sectional view of three phase squirrel cage induction motor

For simplicity, the induction motor considered will have the following assumptions:

- Symmetrical four pole, three phase windings.
- The slotting effects are neglected.
- The permeability of the iron paths is infinite.
- The flux density is radial in the air gap.
- The effects of anisotropy, magnetic saturation, iron losses and eddy currents are neglected.
- In many cases, especially when considering steady state, the currents and voltages are taken to be sinusoidal.
- The rotor is of a squirrel cage type.

A.1.2. Equivalent representation and vector formulation

The machine is represented by three-phase equivalent circuit associated to the stator and to the rotor as shown in **Figure.A.2**.

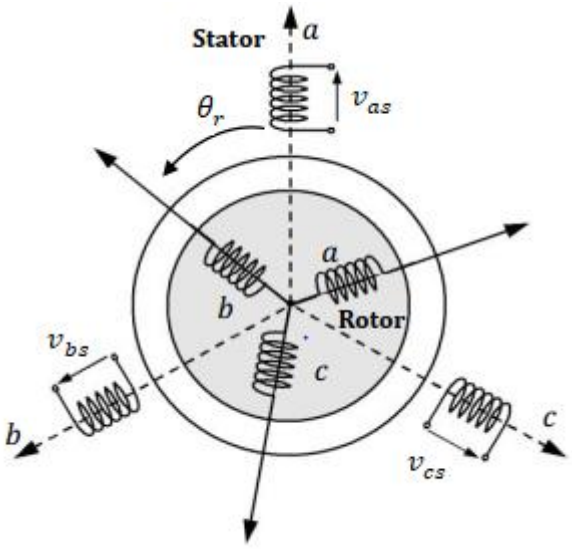

Figure.A.2 Induction motor equivalent structure.

The studied machine is described in the space by three identical windings for the stator phases whose are distant two by two of an electrical angle equal to **2π/3**. In addition, three rotor windings whose axes are equally distant between themselves of an electrical angle equal to **2π/3** rotating at the mechanic speed ω_r. The modeling process consists of applying the electromagnetic laws to the different windings and the motion equation to the rotor carrying the load [12]. The application of the electromagnetic laws yields to six voltage equations and six

A.1.2.1. Voltage equations

By applying Kirchhoff's law to each coil of the stator and rotor windings, we obtain the following:

$$[v_{abcs}] = [R_s][i_{abcs}] + \frac{d}{dt}[\psi_{abcs}] \quad \text{(A.1)}$$

$$[v_{abcr}] = 0 = [R_r][i_{abcr}] + \frac{d}{dt}[\psi_{abcr}] \quad \text{(A.2)}$$

A.1.2.2. Flux equations

$$[\psi_{abcs}] = [L_s][i_{abcs}] + [M_{sr}][i_{abcr}] \quad \text{(A.3)}$$

$$[\psi_{abcr}] = [L_r][i_{abcr}] + [M_{rs}][i_{abcs}] \quad \text{(A.4)}$$

Where

$$[v_{abcs}] = \begin{bmatrix} v_{as} \\ v_{bs} \\ v_{cs} \end{bmatrix}; \quad [i_{abcs}] = \begin{bmatrix} i_{as} \\ i_{bs} \\ i_{cs} \end{bmatrix}; \quad [\psi_{abcs}] = \begin{bmatrix} \psi_{as} \\ \psi_{bs} \\ \psi_{cs} \end{bmatrix}$$

$$[v_{abcr}] = \begin{bmatrix} v_{ar} \\ v_{br} \\ v_{cr} \end{bmatrix}; \quad [i_{abcr}] = \begin{bmatrix} i_{ar} \\ i_{br} \\ i_{cr} \end{bmatrix}; \quad [\psi_{abcr}] = \begin{bmatrix} \psi_{ar} \\ \psi_{br} \\ \psi_{cr} \end{bmatrix}$$

The subscripts *s* and *r* refer to the stator and the rotor, respectively, and the indices *a*, *b*, and *c* refers to the three phases. A direct consequence of the machine perfect symmetry is that all resistance and inductance matrices are symmetric as given below:

$$[R_s] = \begin{bmatrix} R_s & 0 & 0 \\ 0 & R_s & 0 \\ 0 & 0 & R_s \end{bmatrix}; \qquad [R_r] = \begin{bmatrix} R_r & 0 & 0 \\ 0 & R_r & 0 \\ 0 & 0 & R_r \end{bmatrix}; \quad \text{(A.5)}$$

$$[L_s] = \begin{bmatrix} L_s & M_s & M_s \\ M_s & L_s & M_s \\ M_s & M_s & L_s \end{bmatrix}; \qquad [L_r] = \begin{bmatrix} L_r & M_r & M_r \\ M_r & L_r & M_r \\ M_r & M_r & L_r \end{bmatrix}; \quad \text{(A.6)}$$

With: $L_s = L_{ms} + L_{ls}$, $L_r = L_{mr} + L_{lr}$, $M_s = -\frac{L_{ms}}{2}$, $M_r = -\frac{L_{mr}}{2}$

Where: L_{ms} is the magnetizing inductance, accounts for the flux produced by the respective phases, crosses the airgap and links other windings. L_{ls} is the leakage inductance, accounts for the flux produce by the respective phases, but does not cross the airgap and links only itself.

In addition, based on the given hypothesis above, the mutual inductances between the rotor and the stator are taken as sinusoidal functions of the rotor position $\boldsymbol{\theta_r}$ as following:

$$[M_{sr}] = [M_{rs}]^T = M_{sr} \begin{bmatrix} cos(\theta_r) & cos\left(\theta_r + \frac{2\pi}{3}\right) & cos\left(\theta_r + \frac{2\pi}{4}\right) \\ cos\left(\theta_r + \frac{2\pi}{4}\right) & cos(\theta_r) & cos\left(\theta_r + \frac{2\pi}{3}\right) \\ cos\left(\theta_r + \frac{2\pi}{4}\right) & cos\left(\theta_r + \frac{2\pi}{3}\right) & cos(\theta_r) \end{bmatrix} \quad \text{(A.7)}$$

M_{sr} is the maximal mutual inductance between the stator phase and the rotor phase.

A.1.2.3. Mechanical equation

The rotor motion can be described by the following second order differential equation:

$$J\frac{d\omega_r}{dt} = T_e - T_L - B\omega_r \quad \text{(A.8)}$$

Where:

ω_r, T_e and T_L are the rotor speed, the electromagnetic torque and the load torque respectively. J is the inertia moment and B is the friction coefficient.

A.1.3. Dynamic d-q Model

The stator of induction motor consists of three phase balanced distributed windings with each phase separated from other two windings by 120 degrees in space (Bose 1997). When current flows through these windings, three phase rotating magnetic field is produced. The dynamic behavior of the induction machine is taken into account in an adjustable speed drive system using a power electronics converter. This machine constitutes an element within a feedback loop. Study of the dynamic performance of the machine is complex due to coupling effect of the stator and rotor windings; also the coupling coefficient varies with rotor position. So a set of differential equations with time varying coefficients describe the machine model (Bose 1997).

To derive the dynamic model of the machine, the following assumptions are made:

- No magnetic saturation
- No saliency effects i.e. machine inductance is independent of rotor position
- Stator windings are so arranged as to produce sinusoidal mmf distributions
- Effects of the stator slots may be neglected
- No fringing of the magnetic circuit
- Constant magnetic field intensity, radially directed across the air-gap
- Negligible eddy current and hysteresis effects

A.1.3.1. Space vector representation

The space vector in three-phase system is obtained from the vectorial sum of the three-phase quantities, i.e.:

$$X = \frac{2}{3}\left(x_a + x_b e^{j\frac{2\pi}{3}} + x_c e^{j\frac{4\pi}{3}}\right) = \frac{2}{3}\left(x_a + a.x_b + a^2.x_c\right) \quad \text{(A.9)}$$

Where: $a = e^{j\frac{2\pi}{3}} = \cos\frac{2\pi}{3} + j\sin\frac{2\pi}{3}$

The space vector X may represent the motor variables (e.g. current, voltage, and flux). The vector control principle on AC machines takes advantages of transforming the variables from the physical three-phase *abc* system to a stationary frame $\alpha\beta$, or rotating frame *dq*.

A.1.3.2. Axes Transformation

A.1.3.2.1. Clarke Transformation (abc to $\alpha\beta$)

The sinusoidal three-phase variables can be represented as a space vector expressed on a two orthogonal axis ($\alpha\beta$). It is more convenient to align the α-axis with a-axis for simplicity purposes, as shown in **Figure**.**1.3**.

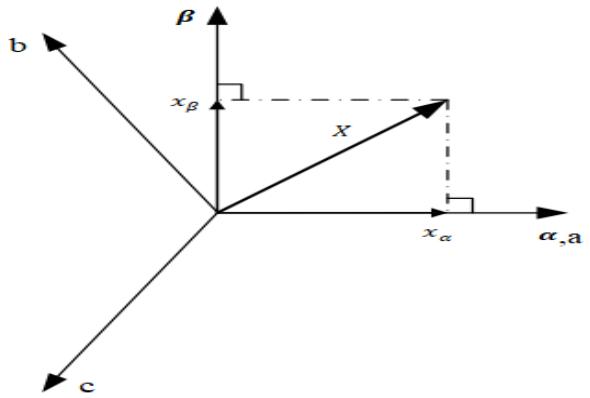

Figure.A.3 Stator current vector $\alpha\beta$ components

In the stationary two-phase system, the space vector is defined as:

$$X = x_\alpha + jx_\beta \quad \text{(A.10)}$$

The space vector in three-phase system must equal to the space vector in two-phase system, hence by comparing (1) and (2) the equivalence between the two systems is obtained:

$$x_\alpha = R_e\left\{\frac{2}{3}[x_a + ax_b + a^2x_c]\right\} = \frac{2}{3}\left(x_a - \frac{1}{2}x_b - \frac{1}{2}x_c\right) \quad \text{(A.11)}$$

$$x_\beta = I_m\left\{\frac{2}{3}[x_a + ax_b + a^2x_c]\right\} = \frac{1}{\sqrt{3}}(x_b - x_c) \quad \text{(A.12)}$$

Hence, in matrix form the $\alpha\beta$ transformation is given by

$$\begin{bmatrix} x_\alpha \\ x_\beta \end{bmatrix} = \begin{bmatrix} \frac{2}{3} & -\frac{1}{3} & -\frac{1}{3} \\ 0 & \frac{1}{\sqrt{3}} & -\frac{1}{\sqrt{3}} \end{bmatrix} \begin{bmatrix} x_a \\ x_b \\ x_c \end{bmatrix} \quad \text{(A.13)}$$

To make the $\alpha\beta$ transformation invertible a third row is added as shown below

$$\begin{bmatrix} x_\alpha \\ x_\beta \\ x_0 \end{bmatrix} = \begin{bmatrix} \frac{2}{3} & -\frac{1}{3} & -\frac{1}{3} \\ 0 & \frac{1}{\sqrt{3}} & -\frac{1}{\sqrt{3}} \\ \frac{1}{3} & \frac{1}{3} & \frac{1}{3} \end{bmatrix} \begin{bmatrix} x_a \\ x_b \\ x_c \end{bmatrix} \quad \text{(A.14)}$$

The third row represents the zero-sequence component which under balanced conditions is null, i.e.:

$$x_0 = x_a + x_b + x_c = 0 \quad \text{(A.15)}$$

Then the $\alpha\beta$ transformation and its invers is given by

$$x_{\alpha\beta 0} = T_{abc}.x_{abc} \qquad x_{abc} = T_{abc}^{-1}.x_{\alpha\beta 0}$$

$$T_{abc} = \begin{bmatrix} \frac{2}{3} & -\frac{1}{3} & -\frac{1}{3} \\ 0 & \frac{1}{\sqrt{3}} & -\frac{1}{\sqrt{3}} \\ \frac{1}{3} & \frac{1}{3} & \frac{1}{3} \end{bmatrix} \qquad T_{abc}^{-1} = \begin{bmatrix} 1 & 0 & 1 \\ -\frac{1}{2} & \frac{\sqrt{3}}{2} & 1 \\ -\frac{1}{2} & -\frac{\sqrt{3}}{2} & 1 \end{bmatrix} \quad \text{(A.16)}$$

Hence, the currents, voltages, and flux in two-phase system ca be obtained the same way as follow:

$$v_{\alpha\beta s} = T_{abc}.x_{abcr} \quad \text{(A.17)}$$

$$v_{\alpha\beta r} = T_{abc}.x_{abcs} \quad \text{(A.18)}$$

$$i_{\alpha\beta s} = T_{abc}.i_{abcs} \quad \text{(A.19)}$$

$$i_{\alpha\beta r} = T_{abc}.i_{abcr} \quad \text{(A.20)}$$

$$\psi_{\alpha\beta s} = T_{abc}.\psi_{abcs} \quad \text{(A.21)}$$

$$\psi_{\alpha\beta r} = T_{abc}.\psi_{abcr} \quad \text{(A.22)}$$

Where s denotes stator quantities and r denotes rotor quantities and: $i_{\alpha\beta} = i_\alpha + ji_\beta$, $\psi_{\alpha\beta} = \psi_\alpha + j\psi_\beta$

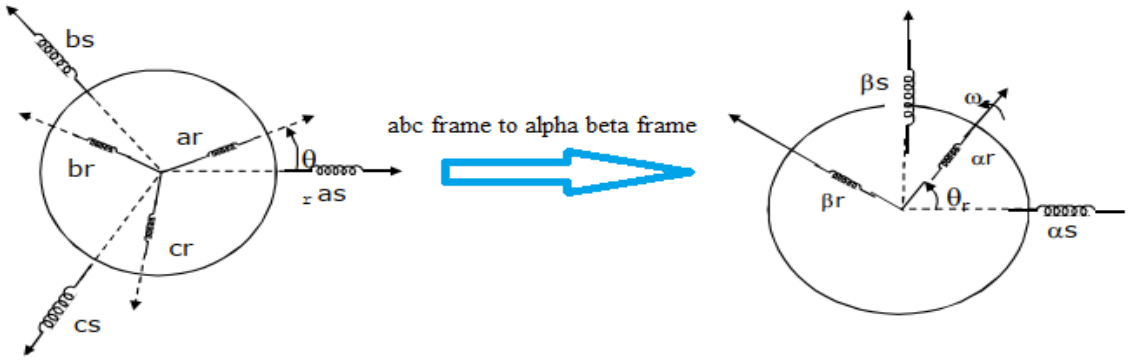

Figure.A.4 Clarke transformation

Hence the voltage equations in the $\alpha\beta$ frame are given as:

$$v_s = R_s i_s + d(\psi_s)/dt = R_s i_{\alpha\beta s} + d(\psi_{\alpha\beta s})/dt \quad \text{(A.23)}$$

$$v_r = R_r i_r + d(\psi_r)/dt = R_s i_{\alpha\beta r} + d(\psi_{\alpha\beta r})/dt \quad \text{(A.24)}$$

Wherev_s, v_r, i_s, i_r, ψ_s *and* ψ_r are space vectors representation of stator and rotor quantities.

Where $i_{\alpha\beta} = i_\alpha + ji_\beta$ and $\psi_{\alpha\beta} = \psi_\alpha + j\psi_\beta$

A.1.3.2.2. Park transformation ($\alpha\beta$ to dq)

In the late 1920s, **R.H. Park** introduced a new approach to electric machine analysis, where he formulated a change of variables associated with fictitious windings rotating with the rotor angular speed ω_e hence, the *dq* quantities can be obtained simply by multiplying the $\alpha\beta$ quantities by the rotating phasor $\boldsymbol{e^{-j\theta_e}}$ (i.e. He referred the stator and rotor variables to a reference frame fixed on the rotor) as shown in **Figure.A.5**.

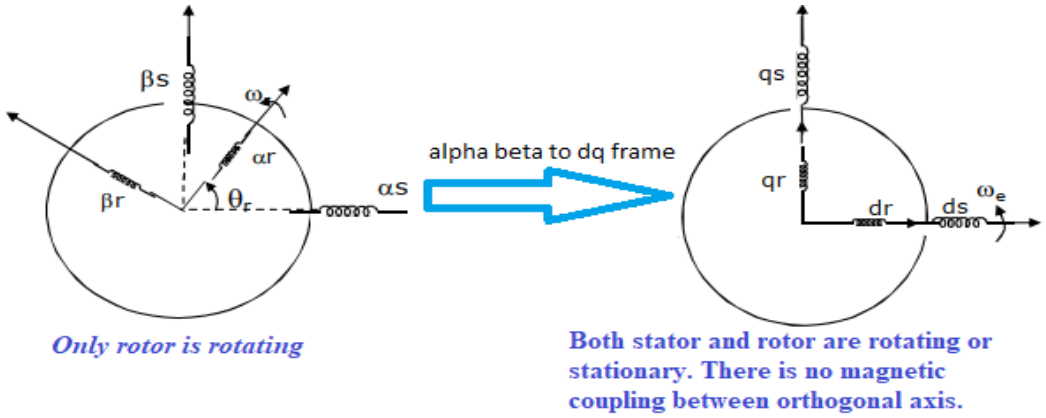

Figure.A.5 Park transformation

From the rotor point of view, all the variables can be observed as constant values. Park's transformation is a revolution in machine analysis, has the unique property of eliminating all time varying inductances from the voltage equations of three-phase ac machines due to the rotor spinning.

The transformation T_e from $\alpha\beta$ to *dq* reference frame and its inverse T_e^{-1} is given by

$$T_e = \begin{bmatrix} \cos(\theta_e) & \sin(\theta_e) \\ -\sin(\theta_e) & \cos(\theta_e) \end{bmatrix} \qquad T_e^{-1} = \begin{bmatrix} \cos(\theta_e) & -\sin(\theta_e) \\ \sin(\theta_e) & \cos(\theta_e) \end{bmatrix} \tag{A.25}$$

The voltages, current and fluxes in *dq* frame are given by:

$$v_{dqs} = T_e . x_{\alpha\beta r} \tag{A.26}$$

$$v_{dqr} = T_e . x_{\alpha\beta s} \tag{A.27}$$

$$i_{dqs} = T_e . i_{\alpha\beta s} \tag{A.28}$$

$$i_{dqr} = T_e . i_{\alpha\beta r} \tag{A.29}$$

$$\psi_{dqs} = T_e . \psi_{\alpha\beta s} \tag{A.30}$$

$$\psi_{dqr} = T_e . \psi_{\alpha\beta r} \tag{A.31}$$

Finally, the *dq* model voltages equations of IM are given as:

$$\begin{cases} v_{ds} = R_s i_{ds} + \frac{d\psi_{ds}}{dt} - \omega_e \psi_{qs} \\ v_{qs} = R_s i_{qs} + \frac{d\psi_{qs}}{dt} + \omega_e \psi_{ds} \\ v_{dr} = R_r i_{ds} + \frac{d\psi_{dr}}{dt} - (\omega_e - \omega_r)\psi_{qr} \\ v_{qr} = R_r i_{qs} + \frac{d\psi_{dr}}{dt} + (\omega_e - \omega_r)\psi_{dr} \end{cases} \quad \text{(A.32)}$$

Where

$\omega_e = \frac{d\theta_e}{dt}$; $\omega_r = \frac{d\theta_r}{dt}$;

Similarly the flux equations are given by

$$[\psi_{dqs}] = L_s[i_{dqs}] + M_{sr}[i_{dqr}] \quad \text{(A.33)}$$

$$[\psi_{dqr}] = L_r[i_{dqr}] + M_{rs}[i_{dqs}] \quad \text{(A.34)}$$

A.1.3.2.1. Mechanical equation

The dynamic equation of the IM is given by the following:

$$J\frac{d\omega_r}{dt} = T_e - T_L - B\omega_r$$

The electromagnetic torque is calculated in (*d*, *q*) frame using the electric power and the rotor speed, and then the expression of torque basing on power preserving Park transformation is given by:

$$T_e = \frac{3}{2}\frac{p}{2}\frac{L_m}{L_r}\left(\psi_{dr} i_{qs} - \psi_{qr} i_{ds}\right) \quad \text{(A.35)}$$

Where L_m is the magnetizing inductance given by: $L_m = \frac{3}{2}M_{sr}$

The electromagnetic torque can also be expressed in the following term:

$$T_e = \frac{3}{2}\frac{p}{2}\left(\psi_{ds} i_{qs} - \psi_{qs} i_{ds}\right) \quad \text{(A.36)}$$

Where ***p*** is the number of pole pairs of the IM.

The model of the induction machine expressed in the rotating frame (*d*, *q*) is often used for the field oriented control design; contrariwise, the direct torque control uses the fixed (stationary) frame (α, β).

A.2. Speed regulation in DTC strategy

Selection of the PI controller parameters will influence the speed response, its settling time, overshoot value and load torque rejection, so they should be adjusted to have optimal response. However, the design of these gains cannot achieve all these characteristics simultaneously as reported in [32-33].To design the PI controller, the schematic diagram of the speed controller of the IM drive is illustrated in **Figure.A.6**.

The dynamic equation and the transfer function using Laplace transform of the speed loop are given as following:

$$\frac{d\omega_r}{dt} = -\frac{B}{J}\omega_r + \frac{T_e}{J} - \frac{1}{J}T_L \tag{A.37}$$

$$G_{\omega_r}(s) = \frac{\omega_r(s)}{T_e(s) - T_L(s)} = \frac{1}{Js+B} \tag{A.38}$$

Whereas the transfer function of the PI controller is defined as

$$G_{PI}(s) = K_p + \frac{K_i}{s} \tag{A.39}$$

K_p and K_i are the proportional and integral gains.

s is Laplace operator.

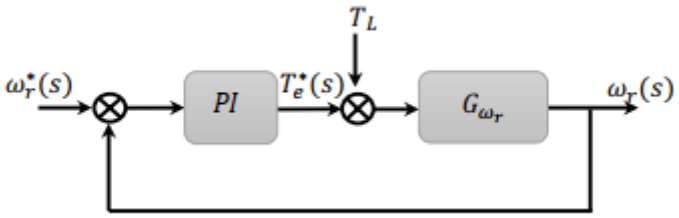

Figure.A.6. Speed control loop

By considering the load torque T_L as a disturbance, and set it to zero, the open loop transfer function (TF) is given as

$$G_{\omega_r\,OL|T_L=0}(s) = \frac{G_{\omega_r}(s)}{G^*_{\omega_r}(s)} = \frac{K_p(s+\frac{K_i}{K_p})}{(Js+B)s} \tag{A.40}$$

For closed loop the TF is given as

$$G_{\omega_r}(s) = \frac{\frac{K_p s + K_i}{J}}{s^2 + \frac{(K_p + B)}{J} s + \frac{K_i}{J}} \quad \text{(A.41)}$$

By identification member to member, the denominator of the equations (A.33) with the canonical form of second order system given in (A.34):

$$G_{\omega_r}(s) = \frac{1}{s^2 + 2\zeta\omega_n s + \omega_n^2} \quad \text{(A.42)}$$

Where ω_n is the natural frequency and ζ is the damping coefficient, we obtain:

$$\begin{cases} \frac{K_i}{J} = \frac{1}{\omega_n^2} \\ \frac{(K_p + B)}{J} = 2\zeta\omega_n \end{cases}$$

The gains are determined for a damping coefficient of 1.

References

[1] I. Takahashi and T. Noguchi, “A new quick-response and high-efficiency control strategy of an induction motor,” *IEEE Trans. Ind. Appl.*, vol. 22, no.5,pp.820–827,Sep.1986.

[2] Y. Zhang and J. Zhu, “Direct torque control of permanent magnet synchronous motor with reduced torque ripple and commutation frequency,” *IEEE Trans. Power Electron.*, vol.26,no.1,pp.235–248,Jan.2011.

[3] A. B. Jidin, N. R. B. N. Idris, A. H. B. M. Yatim, M. E. Elbuluk, and T. Sutikno, “A wide-speed high torque capability utilizing over modulation strategy in DTC of induction machines with constant switching frequency controller,” *IEEE Trans. Power Electron.*, vol. 27, no. pp. 2566–2575,May2012.

[4] J. K. Kang, D. W. Chung, and S. K. Sul, “Direct torque control of induction machine with variable amplitude control of flux and torque hysteresis bands,” in *Proc. Int. Elect. Mach. Drives Conf.*, Seattle, Washington, May 1999,pp.640–642.

[5] K. B. Lee and F. Blaabjerg, “Sensorless DTC-SVM for induction motor driven by a matrix converter using a parameter estimation strategy,” *IEEE Trans. Ind. Electron.*,vol.55,no.2,pp.512–521,Feb.2008.

[6] Z. Zhifeng, T. Renyuyan, B. Boadong, and X. Dexin, “Novel direct torque control based on space vectormodulation with adaptive stator flux observer for induction motors,” *IEEE Trans. Magn.*, vol. 48, no. 8, pp. 3133–3136, Aug.2010.

[7] J. Beerten, J. Verveckken, and J. Driesen, “Predictive direct torque control for flux and torque ripple reduction,” *IEEE Trans. Ind. Electron.*, vol. 57, no.1,pp.404–412,Jan.2010.

[8] H. Zhu, X. Xiao, and Y. Li, “Torque ripple reduction of the torque predictive control scheme for permanent-magnet synchronous motors,” *IEEE Trans. Ind. Electron.*, vol. 59, no.2,pp.871–877,Feb.2012.

[9] S. K. Sahoo, S. Dasgupta, S. K. Panda, and J. X. Xu, “A Lyapunov function-based robust direct torque controller for a switched reluctance motor drive system,” *IEEE Trans. Power Electron.*, vol. 27, no. 2, pp. 555–564,Feb.2012.

[10] M. N. Uddin and M. Hafeez, “FLC-based DTC scheme to improve the dynamic performance of an IM drive,” *IEEE Trans. Ind. Appl.*, vol. 48, no.2,pp. 823 831,Mar./Apr.2012.

[11] Haitham Abu-Rub, Atif Iqbal, Jaroslaw Guzinski “High Performance Control of AC Drives with MATLAB/Simulink Models, First Edition. Published 2012 by John Wiley & Sons Ltd.

[12] Fouad Giri “AC electric motors control advanced design techniques and applications” John Wiley & Sons, Ltd, 2013

[13] Flemming Abrahamsen “Energy Optimal Control of Induction Motor Drives” Ph.D. thesis, Aalborg University, Denmark, 2000.

[14] C. Martins and A. Carvalho, "Technological trends in induction motor electrical drives", in IEEE Porto Power Tech Proceedings 2001.

[15] G. S. Buja and M. P. Kazmierkowski, "Direct torque control of PWM inverter-fed AC motors - a survey," IEEE Trans. Ind. Electronics, vol. 51, pp. 744-757, 2004.

[16] K. Hasse, “Drehzahlgelverfahren für schnelle umkehrantriebe mit stromrichtergespeisten asynchron-kurzschlusslaufer-motoren,” *Reglungstechnik*, vol.n20, pp. 60–66, 1972.

[17] F. Blaschke, “The principle of field orientation as applied to the new transvector closed-loop control system for rotating machines,” *Siemens Review*, vol. 39, no. 5, pp. 217–220, 1972.

[18] Takahashi, T.Noguchi, “A new quick-response and high-efficiency control strategy of an induction motor,” IEEE Trans. on Ind. Appl., Vol.22, No.5, pp.820-827, 1986.

[19] M. Depenbrock, "Direct Self Control (DSC) of Inverter Fed Induction Machine", IEEE Trans. on Power Electronics, Vol. 3, No.4, pp.420-429, 1988.

[20] Mihai Comanescu “Fux and speed estimation techniques for sensorless control of induction motors” Ph.D. thesis, The Ohio State University USA, 2005.

[21] I. M. Alsofyani and N. R. N. Idris, "A review on sensorless techniques for sustainable reliablity and efficient variable frequency drives of induction motors," J. Renewable and Sustainable Energy Reviews, vol. 24, pp. 111-121, 2013.

IEEE Trans. on Power Electronics, Vol. 3, No.4, pp.420-429, 1988

[22] Farid TAZERART “Étude, Commande et Optimisation des Pertes d'Énergie d'une Machine à Induction Alimentée par un Convertisseur Matriciel” Ph.D. thesis, Bejaia University, Algeria, 2016.

[23] Marcin Żelechowski “Space Vector Modulated – Direct Torque Controlled (DTC SVM) Inverter – Fed Induction Motor Drive” Ph.D. thesis, Warsaw University of Technology, Warsaw, Poland, 2005.

[24] N. R. N. Idris and A. H. M. Yatim, "Direct torque control of induction machines with constant switching frequency and reduced torque ripple," IEEE Trans. Ind. Electronics, vol. 51, pp. 758-767, 2004

[25] D. Casadei, F. Profumo, G. Serra, and A. Tani, "FOC and DTC: Two viable schemes for induction motors torque control," IEEE Trans. Power Electron., vol. 17, no. 5, pp. 779–787, 2002.

[26] Dariusz Świerczyński "Direct Torque Control with Space Vector Modulation (DTC-SVM) of Inverter-Fed Permanent Magnet Synchronous Motor Drive" Ph.D. thesis, Warsaw University of Technology, Warsaw, Poland, 2005.

[27] Antoni Arias Pujol "Improvements in direct torque control of induction motors" Ph.D. thesis, Universitat politécnica de Catalunya, Terrassa, 2000.

[28] Z. Zhang, C. Wei, W. Qiao and L. Qu, "Adaptive Saturation Controller-Based Direct Torque Control for Permanent-Magnet Synchronous Machines", IEEE Transactions on Power Electronics, pp. 7112-7122, 2016.

[29] Riad TOUFOUTI, Salima MEZIANE, Hocine BENALLA "Direct torque control strategy of induction motors" acta electrotechnica et informatica vol. 7, no. 1, 2007.

[30] Mohamed Azab and A.L. Orille, "Novel Flux and Torque Control of IM Drive using FSTPI", *in IEEE Proceeding IECON conference,* 2001,pp 1268 -1273.

[31] B. El Badsi, B. Bouzidi, and A. Masmoudi, "DTC scheme for a four-switch inverter-fed induction motor emulating the six-switch inverter operation" IEEE Trans. Power Electron., **28**(7), 3528-3538, Jul. 2013.

[32] Mohamed S. Zaky, "A self-tuning PI controller for the speed control ofbelectrical motor drives," Electric Power Systems Research, vol. 119, pp. 293–303, 2015.

[33] L. Harnefors, S. E. Saarakkala, and M. Hinkkanen, Speed Control of Electrical Drives Using Classical Control Methods, IEEE Transactions On Industry Applications, vol. 49, no. 2, pp. 889-898, 2013.

[34] Power Electronics Handbook - Devices, Circuits, and Applications, 2nd Edition, Muhammad H Rashid.